

台灣顯微鏡學會

第三十五屆學術研討會 104年7月11日 國立台灣大學



日本電子株式会社
捷東股份有限公司

Solutions for Innovation

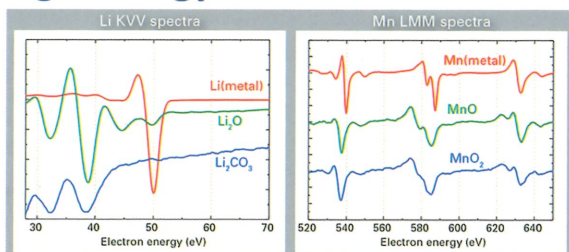
JSM-7800F *Prime* の誕生 Field Emission Scanning Electron Microscope

- Gentle Beam Super High Resolution:
High Resolution of 0.7 nm at 1 kV
- In-lens Schottky *Plus* max beam current:
20 nA at 2kV / 500 nA at 30 kV
- Long-term stability
- Long service life
3-year warranty for emitter



JAMP-9510F Auger Electron Spectrometer

- High spatial resolution of Auger analysis: 8 nm
- Energy resolution: 0.05% to 0.6%
- Chemical state analysis at the nanoscale
with high energy resolution



www.jiedong.com.tw

主辦單位：台灣顯微鏡學會 協辦單位：台灣大學材料科學與工程學系

Founded in 2002, Materials Analysis Technology Inc. (MA-tek) is a leading laboratory in materials analysis (MA). Accompanying with the fast growing pace of business development, MA-tek has successfully expanded to provide Failure Analysis (FA) and Reliability Testing (RT) services as well, which is superior integrated service for customers in various industries. Up to now, MA-tek has set up 6 laboratories and 1 sales office worldwide, providing around-the-clock services in logistic support and technical services.

Our Service Items

Project Based Services

- Training Courses, Lectures
- IP strategic planning
- Patent infringement study
- Benchmark study
- Competitors Analysis
- Design Services

MA / PFA

- Decap, Delayer, Parallel lapping
- SEM / EDX
- TEM / EDX / EELS
- FIB, Circuit editing
- SIMS, SRP
- Auger, XPS, XRD
- Optical profiler
- SCM, AFM
- FTIR, Raman

EFA / ESD

- X-ray radiography
- SAT
- EMMI / InGaAs, OBIRCH
- Themos-mini
- C-AFM
- Passive voltage contrast
- ESD / Latch-up testing
- Wire bonding, packaging

Reliability Tests

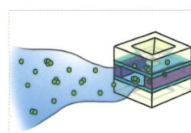
- HAST, LTST
- THST, PCT / UB-HAST
- TCT, TST
- HTOL, BLT, ELFR
- Reflow Test

◆ Case log-in, please contact: sales@ma-tek.com / +886 3 611 6678 ext.3821 / www.ma-tek.com

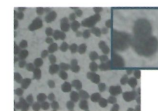
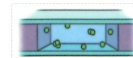


Bio Materials Analysis Technology Inc. (Bio Ma-tek) address the ever demanding needs on the physical and chemical characterization of nano materials in biological systems, Bio Ma-tek rolls out an array of bio-EM sample preparation and image analysis services and a comprehensive list of analytical services following the recommendations in ISO/TR13014.

Specimen kit for observing the original morphology and physical state of nanomaterials in liquid sample by TEM

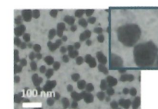
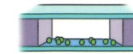


Wet



The loaded liquid sample is sealed and imaged by TEM in the native liquid environment.

Thin Layer



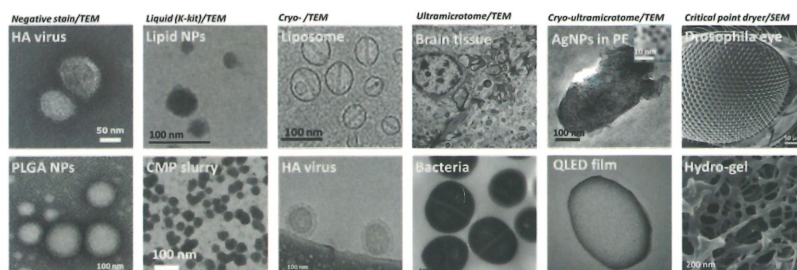
A proprietary sample preparation protocol preserves the original morphology and physical state with improved imaging resolution.

- ✓ US 7,807,979 B2
- ✓ PCI/US2013/049595
- ✓ Anal. Chem. 2012, 84: 6312-6316

Picture shown: Undiluted CMP-slurry directly loaded into K-kit to observe the primary and secondary abrasives by TEM.

Liquid Sample TEM

- Liquid Sample TEM Service and Sales
- Bio-sample and Bio-materials EM Specimen Preparation
- Other Electron Microscopy Analysis : Liquid 、 Cryo 、 Gel 、 Solid 、 etc.

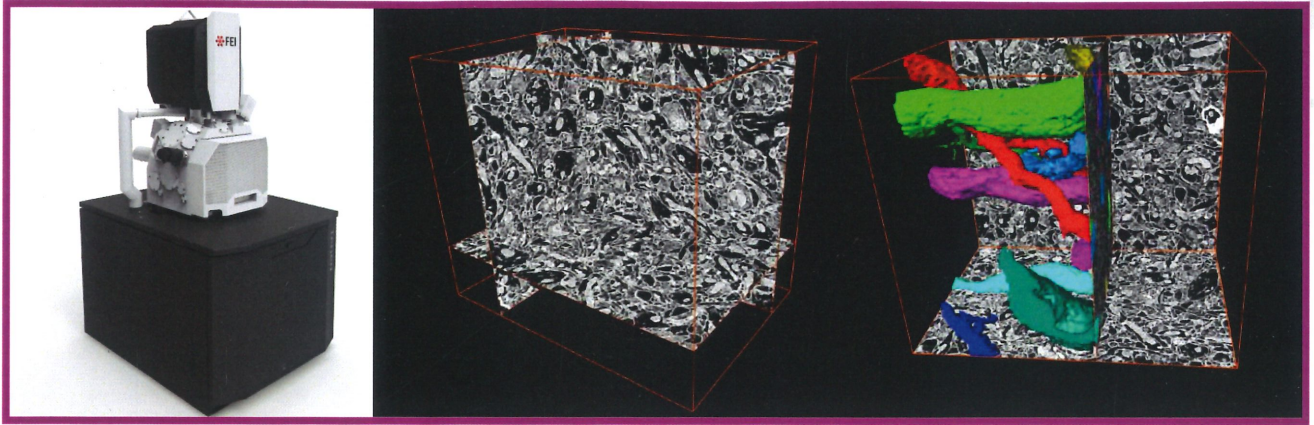



Other TEM Specimen Preparation



超泰科技有限公司
E.B. TECH CO., LTD.

專業的電子顯微鏡, 材料分析儀器, 耗材, 相關設備代理商
Electron Microscope, Analysis instruments, Sample preparation tools



 FEI™ 高低真空掃描式電子顯微鏡; 3D影像立體重構 (Serial Block Face)



場發射掃描/穿透式電子顯微鏡
低溫冷凍樣品製備 (Cryo-TEM)



電漿清洗機 (Plasma Cleaner)
冷凍立體攝影試片座 (Holder)



能量散佈分析儀 (EDS); 電子繞射儀 (EBSD)
聚焦離子束顯微鏡用吸針系統 (Ominiprobe system)



影像擷取元件 (CCD)
試片研磨拋光設備
電子顯微鏡相關設備耗材

台北市光復南路495號7樓之5
TEL: 02-2729-5268
Http://www.ebtech.com.tw

佳佑儀器有限公司

地址：30091 新竹市經國路三段92巷10號12樓
 電話：(03) 530-2385 傳真：(03) 530-6186
 網址：www.jja.com.tw
 E-mail: konica@jja.com.tw

TEM/SEM/金相試片前處理設備耗材

1. 鑽石刀切割機 & 砂輪刀切割機
2. 單盤 & 雙盤 研磨拋光機
3. 熱鑲埋成型機
4. 冷鑲埋 & 熱鑲埋 專用耗材
5. 3M研磨砂紙 & 3M鑽石拋光膜
6. 拋光用氧化鋁粉 & 拋光絨布
7. 鑽石刀片 & 砂輪刀片
8. TEM專用銅環 & 銅網系列
9. SEM專用桌上型鍍金機 & 濺鍍靶材
10. TEM & SEM 試片代測服務(技術諮詢)

光學顯微鏡組 & 影像擷取量測設備

1. 客製化架設CCD觀測鏡頭
2. 長工作距離光學變焦顯微鏡
3. 立體顯微鏡
4. 金相觀測光學顯微鏡
5. 三次元工具量測顯微鏡
6. 彩色 & 黑白 數位式CCD (USB系統)
7. 影像擷取 & 2.5D量測模組
8. LED & 鹵素光纖光源
9. 各式載物平台設計規劃

實驗室儀器 & 客製化設備

1. 接觸角量測系統
2. 特殊冶具加工設計
3. ITO玻璃切割機
4. 旋轉塗佈機
5. 各類型烘箱 & 管型高溫爐
6. 不鏽鋼材質手套箱
7. 電子分析天秤 & 電磁加熱攪拌機
8. 實驗儀器客製化設計開發
9. 實驗室專用實驗桌 & 排煙櫃體設計規劃

奈米壓印模具設計 & 電性量測設備

1. 客製化奈米壓印模具設計開發
2. 四點探針量測系統/Probe Station
3. 半導體元件電性量測系統
4. 鎢鋼探針
5. 各式針座專用針桿 & 訊號傳輸線材

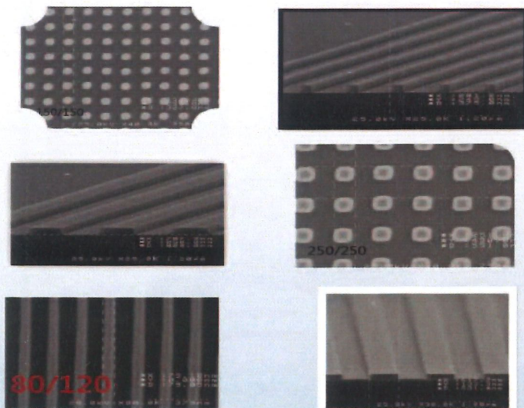
Nanoimprint

客製化奈米壓印模具設計

奈米壓印微影技術

其解析度不受限於光的散射、繞射等光學效應影響並省下製作費用，因為奈米壓印只需要製作壓印模具，即可進行多次且快速的印刷及圖形轉移

模具成品示意圖如下



模具規格

| 壓印圖案規格 Pattern | | | 模具規格 Mold | | |
|----------------------------|-------------|---------------|------------------|---------------------|----------------|
| 圖形尺寸 Critical Dimension | 深度 Depth | 圖案 Feature | 模具材料 Material | 模具大小 Sample Size | 編號 Part No. |
| 50um ~ 3um | 2.0um | Line/Space | Silicon/Glass | 2cm*2cm | SM-M(1) |
| | 1.0um | Hole | | | SM-M(2) |
| | 0.5um | Dot | | | SM-M(3) |

| 壓印圖案規格 Pattern | | | 模具規格 Mold | | |
|----------------------------|-------------|---------------|------------------|---------------------|----------------|
| 圖形尺寸 Critical Dimension | 深度 Depth | 圖案 Feature | 模具材料 Material | 模具大小 Sample Size | 編號 Part No. |
| 3um ~ 400nm | 400nm | Line/Space | Silicon/Glass | 2cm*2cm | SS-M(1) |
| | 300nm | Hole | | | SS-M(2) |
| | 200nm | Dot | | | SS-M(3) |

| 壓印圖案規格 Pattern | | | 模具規格 Mold | | |
|----------------------------|-------------|---------------|------------------|---------------------|----------------|
| 圖形尺寸 Critical Dimension | 深度 Depth | 圖案 Feature | 模具材料 Material | 模具大小 Sample Size | 編號 Part No. |
| 400nm ~ 100nm | 300nm | Line/Space | Silicon/Glass | 2cm*2cm | SN-M(1) |
| | 200nm | Hole | | | SN-M(2) |
| | 100nm | Dot | | | SN-M(3) |

客製化



~歡迎來電洽詢~

TEM材料分析

技術能量達10奈米之實驗室

先進製程檢測 最佳解決方案



應用領域：
IC產業、LED產業、面板產業、TFT-LCD產業、
太陽電池產業、奈米材料研究等。

宜特材料分析三大保證：

1. 已完成知名晶圓廠, LED磊晶廠和面板廠的分析試樣, 獲得客戶肯定與高度評價。
2. TEM權威鮑忠興等多位博士專家, 為您提供最頂尖的服務。
3. 全天候三班制24小時運作, 全面縮短交期, 產能大躍進。

Advanced Logic Device Analysis

High resolution TEM/EDS analysis on advanced MOS devices

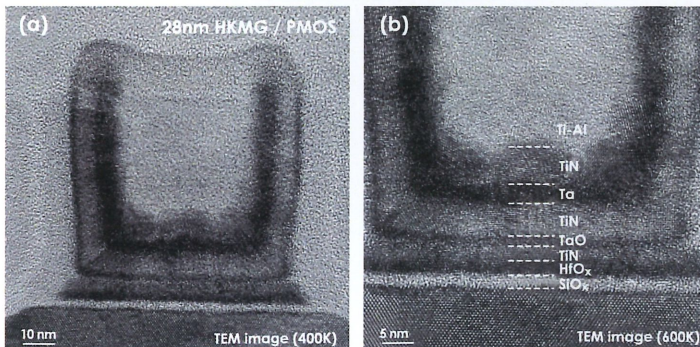


Figure (a) and (b): BF TEM image of a 28nm HKMG PMOS device.

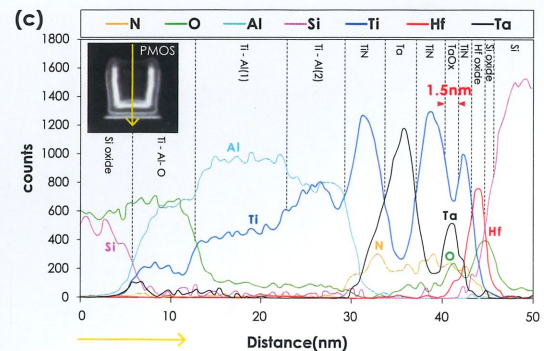


Figure (c): EDS lin-scan results of the gate stack. The 1.5nm-thick Ta layer can be well examined.

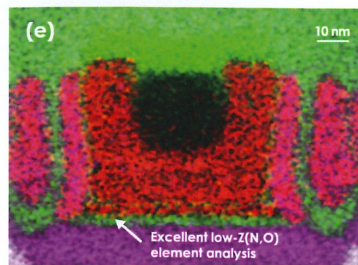
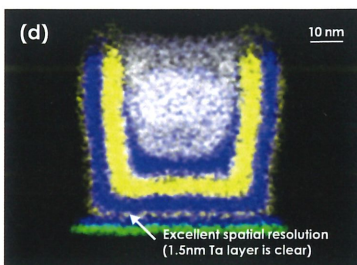


Figure (d) and (e) : EDS mapping results of the 28nm HKMG PMOS device. The 1.5nm-thick Ta layer and some O and N-contained layers can be well examined.

*以上影像皆由JEOL JEM-2800 場發射TEM機台取得。

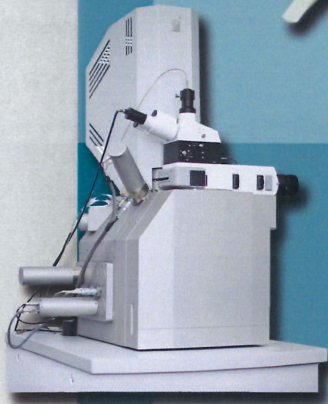


PERFORMANCE IN NANOSPACE

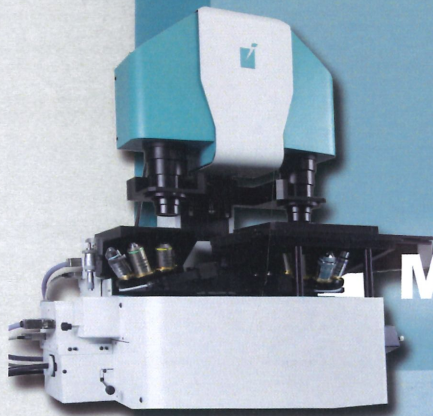
總代理 皓睿科技



Tungsten/ LaB6 **SEM**



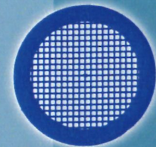
Schottky **FE-SEM**
Integration of confocal *Raman imaging*
with the ultra-high resolution SEM.



Ga+ LMIS **FIB**
Perform *SIMS analysis in-situ*
with access to all features of the FIB.

Xe Plasma **FIB**
Fast more than 50 times
compared with Gallium FIB.

Multimodal Holographic Microscope
Quantitative phase imaging (QPI)
based on patented technology of
Coherence-controlled holographic
microscopy.



皓睿科技

www.tescan.com / www.hsictech.com

電話: 02-2555-5888(代表號)

地址: 台北市大同區長安西路56號8樓

議程

104年7月11日 台灣大學博理館

| | |
|----------------------|---|
| 09:30 – 10:00 | 報到 |
| 10:00 – 10:10 | 開幕、致詞 |
| 10:10 – 11:30 | 專題演講 主持人：楊哲人教授、高甫仁教授 |
| 10:10 – 10:50 | Applications of Electron Microscopy in the Investigations on Nanoscale Copper and Copper Compounds 陳力俊教授 |
| 10:50 – 11:30 | Route 2014: the New Avenue to Nanoscopy 2.0. Prof. Alberto Diaspro |
| 11:30 – 12:00 | 會員大會 |
| 12:00 – 13:30 | 午餐、論文壁報時間 |
| 13:30 – 14:30 | 邀請演講 主持人：周苡嘉教授 |
| 13:30 – 13:50 | Dynamic Evolution of Conducting Nanofilament in Resistive Switching Memories 吳文偉教授 |
| 13:50 – 14:10 | Atomic-Column-by-Atomic-Column Spectroscopy for Emergent Phenomena at Oxide Interfaces 朱明文博士 |
| 14:10 – 14:30 | New Developments for Material Physics in Electron Microscopy Mr. Yukihiro Kondo |
| 14:30 – 14:50 | Coffee break |
| 14:50 – 16:10 | 邀請演講 主持人：陳香君教授 |
| 14:50 – 15:10 | Electron Microscopy 4.0: How Integrating Technologies Help Cure Diseases 余涌博士 |
| 15:10 – 15:30 | Remodeling of Calcium Signaling in Tumor Progression 沈孟儒教授 |
| 15:30 – 15:50 | Cell-to-cell Spread of Dengue Viruses 陳維鈞教授 |
| 15:50 – 16:10 | Nanoparticles for <i>in vitro</i> and <i>in vivo</i> Optical Imaging 陳培菱博士 |
| 16:10 – 17:00 | 頒獎、摸彩、閉幕 |

目錄

| | | |
|----|--|----|
| 一、 | 第十六屆理、監事名錄 | 1 |
| 二、 | 第三十五屆台灣顯微鏡學會學術研討會邀請演講 | |
| | Applications of Electron Microscopy in the Investigations on Nanoscale Copper and Copper Compounds 陳力俊教授 | 2 |
| | Route 2014: the New Avenue to Nanoscopy 2.0. Prof. Alberto Diaspro | 4 |
| | Dynamic Evolution of Conducting Nanofilament in Resistive Switching Memories 吳文偉教授 | 6 |
| | Atomic-Column-by-Atomic-Column Spectroscopy for Emergent Phenomena at Oxide Interfaces 朱明文博士 | 7 |
| | New Developments for Material Physics in Electron Microscopy Mr. Yukihiro Kondo | 8 |
| | Electron Microscopy 4.0: How Integrating Technologies Help Cure Diseases 余涌博士 | 9 |
| | Remodeling of Calcium Signaling in Tumor Progression 沈孟儒教授 | 10 |
| | Cell-to-cell Spread of Dengue Viruses 陳維鈞教授 | 11 |
| | Nanoparticels for <i>in vitro</i> and <i>in vivo</i> Optical Imaging 陳培菱博士 | 12 |
| 三、 | 學生論文壁報目錄 | 13 |
| 四、 | 顯微攝影作品目錄 | 31 |

台灣顯微鏡學會

第十六屆理、監事名錄

| | | | |
|------|-----|-------------------|-------|
| 理事長 | 楊哲人 | 台灣大學材料科學與工程學系 | 教授 |
| 副理事長 | 黃玲瓏 | 台灣大學生命科學系 | 教授 |
| 秘書長 | 溫政彥 | 台灣大學材料科學與工程學系 | 助理教授 |
| 常務理事 | 薛富盛 | 中興大學材料科學與工程學系 | 教授 |
| | 陳福榮 | 清華大學工程與系統科學系 | 教授 |
| | 劉康庭 | 友聯光學股份有限公司 | 董事長 |
| 理事 | 胡宇光 | 中央研究院物理研究所 | 研究員 |
| | 陳香君 | 台灣大學生命科學系 | 教授 |
| | 張立 | 交通大學材料科學與工程學系 | 教授 |
| | 劉全璞 | 成功大學材料科學及工程學系 | 教授 |
| | 陳淑華 | 台灣大學生命科學系 | 教授 |
| | 朱明文 | 台灣大學凝態科學研究中心 | 研究員 |
| | 章為皓 | 中央研究院化學研究所 | 副研究員 |
| | 謝詠芬 | 閎康科技股份有限公司 | 董事長 |
| | 蔡定平 | 台灣大學物理學系 | 教授 |
| 候補理事 | 李志浩 | 清華大學工程與系統科學系 | 教授 |
| | 高甫仁 | 陽明大學生醫光電研究所 | 教授 |
| | 簡萬能 | 中央研究院植物暨微生物學研究所 | 研究技師 |
| | 薛景中 | 中央研究院應用科學研究中心 | 研究員 |
| | 孫啟光 | 台灣大學電機工程學系 | 教授 |
| | 蘇紘儀 | 台灣積體電路製造股份有限公司 | 處長 |
| 常務監事 | 曾傳銘 | 中央研究院物理研究所 | 研究助技師 |
| 監事 | 羅聖全 | 工業技術研究院 | 研究員 |
| | 鮑忠興 | 宜特科技股份有限公司 | 博士 |
| | 張正 | 中興大學園藝學系 | 教授 |
| | 林招松 | 台灣大學材料科學與工程學系 | 教授 |
| 候補監事 | 劉淦光 | 國家衛生研究院分子與基因醫學研究所 | 研究員 |

Applications of Electron Microscopy in the Investigations on Nanoscale Copper and Copper Compounds

Lih-Juann Chen (陳力俊)*

Department of Materials Science and Engineering, National Tsing Hua University, Hsinchu, Taiwan

*ljchen@mx.nthu.edu.tw

Copper has been in use for at least 10,000 years. Copper alloys, such as bronze and brass, have played important roles in advancing civilization in human history. Bronze artifacts date at least 6,500 years, while examples of brass are known in China for about 2,500 years. In the middle ages, the invention of printing in the 15th century increased the demand for copper because of the ease with which copper sheets could be engraved or etched for use as printing plates. Copper sheathing of the hulls of wooden ships was introduced in the middle of the 18th century to the great benefits of long distance voyages by sea and naval battles. With the electrification of the world, it has been mostly used for electrical wires, both for electrical signal and power transmission and as induction coils for electric motors. It is intriguing that in modern era, Cu-based materials have found new ways into many branches of technology such as Cu metallization in nanoelectronics devices, Cu oxide based superconductors, Cu-In-Ga-Se (CIGS) solar materials etc. Furthermore, discovery of intriguing properties and new applications in contemporary technology for copper and its compounds have continued.

In this presentation, a broad overview of the nanoscale copper and Cu compounds, with particular emphasis in the electron microscope examinations, will be given. Examples will be provided on nanoscale Cu metallization in microelectronics devices (Fig. 1) [1], Cu₂S nanowire array cathode in lithium battery applications, multi-level switching behaviors in Cu₂S nanowire resistive random access memory (ReRAM) devices (Fig. 2) [2], switching devices utilizing facet-dependent electrical conductivity of Cu₂O nanocrystals [3], superlattice Cu₂S-Ag₂S nanowire p-n junctions (Fig. 3) [4].

References

1. K.C. Chen, W.W. Wu, C.N. Liao, L.J. Chen, and K.N. Tu, *Science* **321**, 1066 (2008).
2. P.H. Liu, C.C. Lin, A. Manekkathodi, and L.J. Chen, *Nano Energy* **15**, 362 (2015).
3. Chih-Shan Tan, Shih-Chen Hsu, Wei-Hong Ke, Lih-Juann Chen, and Michael Huang, *Nano Lett.* **15**, 2155 (2015).
4. Chih-Shan Tan, Ching-Hung Hsiao, Shau-Chieh Wang, Pei-Hsuan Liu, Ming-Yen Lu, Michael H. Huang, Hao Ouyang, and Lih-Juann Chen, *ACS Nano* **8**, 9422 (2014).

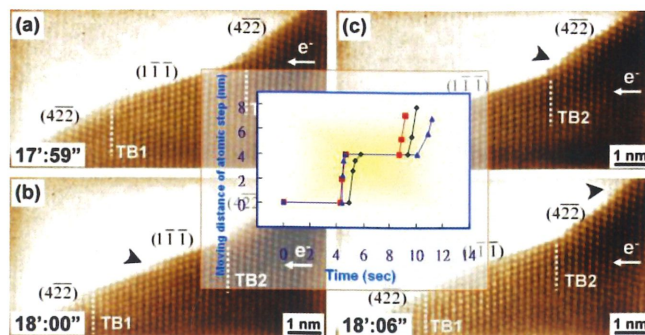


Figure 1. Observation of atomic diffusion at twin-modified grain boundaries in copper.

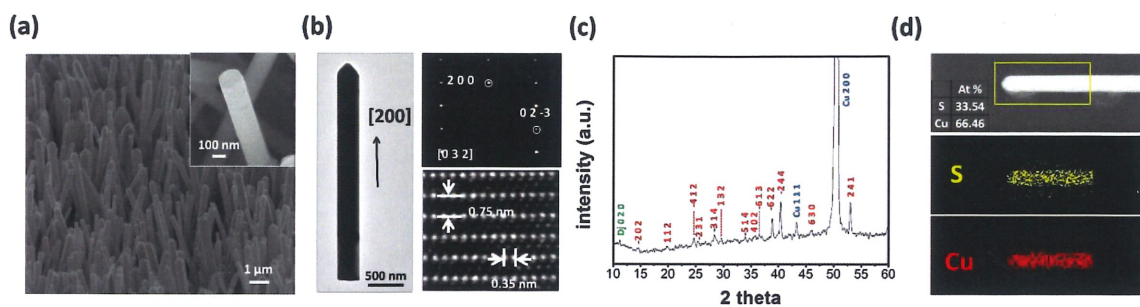


Figure 2. Morphological and structural characterization of Cu_2S nanowires. (a) SEM image, (b) TEM image. Right panels: SAED and HRTEM image. (c) XRD. (d) EDS mapping of the STEM image.

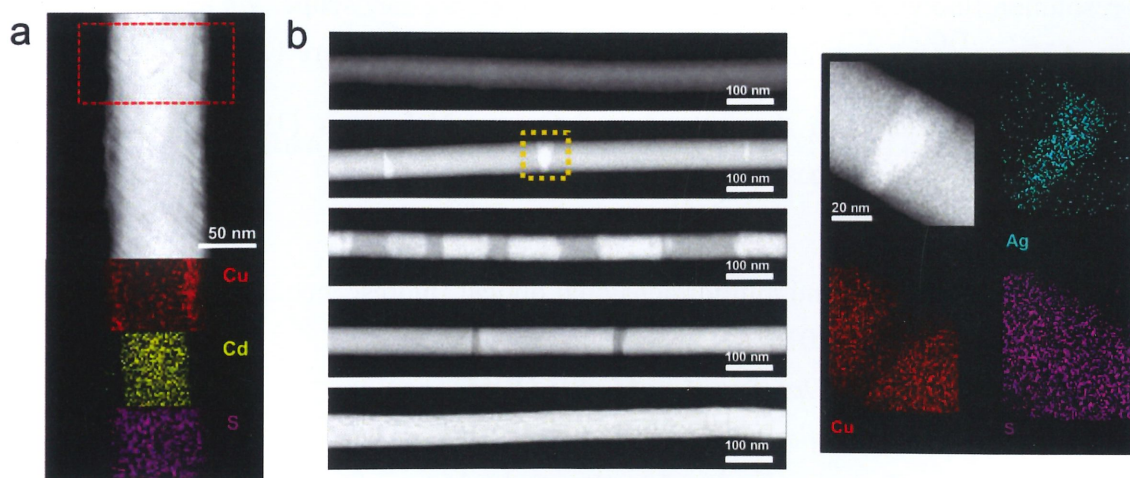


Figure 3. (a) Cu_2S - CdS core-shell structure. (b) HAADF images Cu_2S - Ag_2S superlattice NWs. Right panels: STEM-EDS mapping for the frame region.

Route 2014: the New Avenue to Nanoscopy 2.0.

Alberto Diaspro,* Paolo Bianchini, Francesca Cella Zancchi, Marti Duocastella,
Luca Lanzaò, Colin JR Sheppard, Giuseppe Vicidomini

Nanoscopy and Nikon Imaging Center, Istituto Italiano di Tecnologia;
LAMBS, Department of Physics, University of Genoa; Genoa, Italy

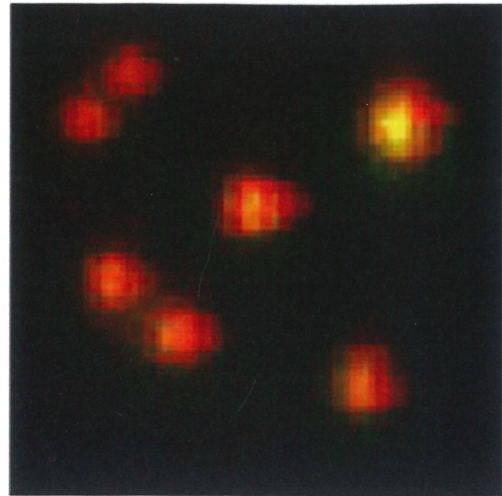
* alberto.diaspro@iit.it

Super-resolution or super resolved fluorescence microscopy, as indicated in the Chemistry Nobel Prize 2014 awarded to Eric Betzig, Stefan W. Hell and William Moerner, includes those microscopy techniques that increase the resolving ability of a light microscope well beyond the classical limits dictated by the diffraction barrier. Several methodologies have been developed over the past several years including saturated structured-illumination microscopy (SSIM), stimulated emission depletion microscopy (STED), photoactivated localization microscopy (PALM), fluorescence photoactivation localization microscopy (FPALM), and stochastic optical reconstruction microscopy (STORM) [1]. It is worth mentioning that the Toraldo di Francia approach related to super-resolution [2] was a fundamental starting point. It is revolutionary today the fact that there is theoretically no limit for capturing details by means of an optical microscope and that, at the very same time, there is the possibility of tuning the spatial resolution according to the scientific question posed [3]. In the style of Johannes Faber referred to the Galileo Galilei's occhialino [4], one can modify the sentence "microscopium nominare libuit" in "nanoscopium nominare libuit" for the super-resolution fluorescence microscope that has become a nanoscope. We already are in the new era of Nanoscopy 2.0 including correlative Nanoscopy [5], figure 1.

This lecture is dedicated to the memory of Osamu Nakamura (1962-2005) and Mats Gustaffson (1960-2011) that passed away too early.

References

1. A. Diaspro, Nanoscopy and multidimensional optical fluorescence microscopy, Chapman and Hall/CRC, London (2010).
2. G. Toraldo di Francia, *J. Opt. Soc. Am.* **45**, 497 (1955).
3. A. Diaspro, *Il Nuovo Saggiatore* **30**, 45 (2014).
4. J. Faber, Letter to Federico Cesi – Accademia dei Lincei, Roma, 13 aprile 1625, in G. Galilei, *Opere*, ed. nazionale a cura di A. Favaro, Firenze, **XIII** 264 (1968).
5. C. Smith, *Nature* **492**, 293 (2012).



Overlap

STED AFM

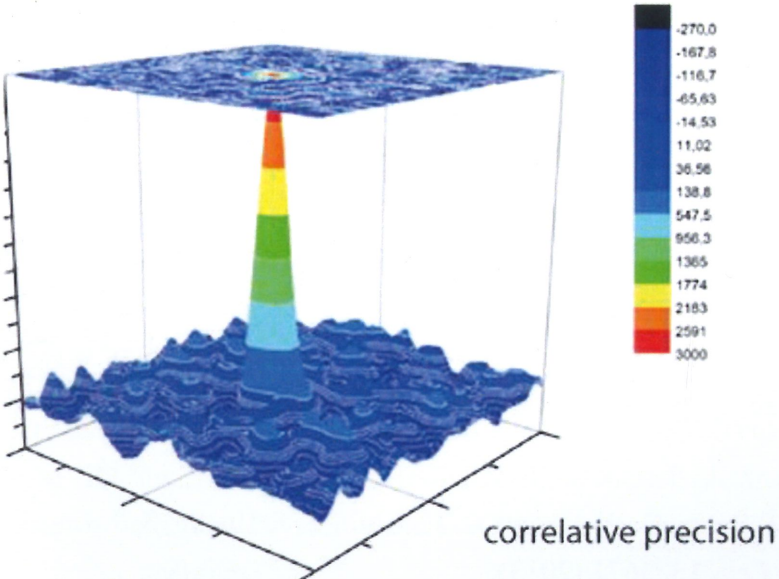


Figure 1. Correlative nanoscopy matching AFM-STED.

Dynamic Evolution of Conducting Nanofilament in Resistive Switching Memories

Jui-Yuan Chen (陳睿遠), Chun-Wei Huang (黃浚璋), Chung-Hua Chiu (邱崇樺), Yu-Ting Huang (黃宇廷), and Wen-Wei Wu (吳文偉)*

Department of Materials Science and Engineering, National Chiao Tung University, Hsinchu, Taiwan

*wwwu@mail.nctu.edu.tw

Resistive random access memory (RRAM) has been considered the most promising next-generation nonvolatile memory. In recent years, the switching behavior has been widely reported, and understanding the switching mechanism can improve the stability and scalability of devices. We designed an innovative sample structure for *in situ* transmission electron microscopy (TEM) to observe the formation of conductive filaments in the MIM(metal/insulator/metal) structure in real time. The corresponding current–voltage measurements help us to understand the switching mechanism of metal oxide film. In addition, high-resolution transmission electron microscopy (HRTEM) and electron energy loss spectroscopy (EELS) have been used to identify the atomic structure and components of the filament/disrupted region, determining that the conducting paths are caused by the conglomeration of metallic phase. The behavior of resistive switching is due to the migration of oxygen ions, leading to transformation between metal-rich phase and metal oxide.

References

1. J. Y. Chen, C. L. Hsin, C. W. Huang, C. H. Chiu, Y. T. Huang, S. J. Lin, W. W. Wu, and L. J. Chen, *Nano Lett.* **13**, 3671 (2013).
2. J. Y. Chen, C. W. Huang, C. H. Chiu, Y. T. Huang, and W. W. Wu, (Submitted).

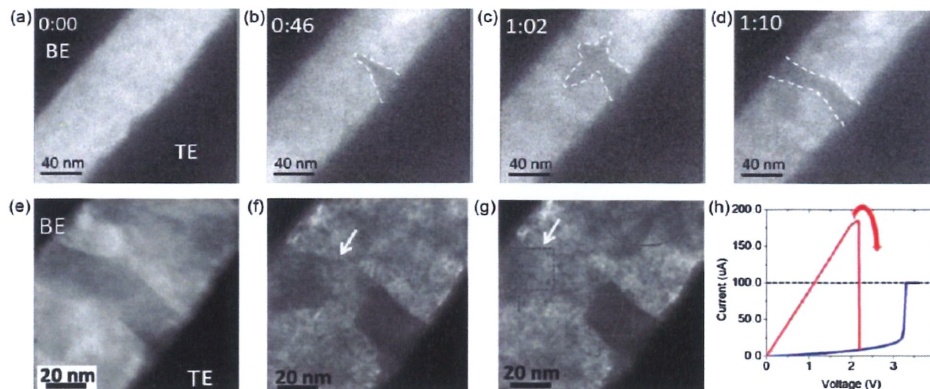


Figure 1. *In situ* TEM images of set and reset process in Pt/ZnO/Pt RRAM device and its corresponding I-V curve.

Atomic-Column-by-Atomic-Column Spectroscopy for Emergent Phenomena at Oxide Interfaces

Ming-Wen Chu (朱明文)*

Center for Condensed Matter Sciences, National Taiwan University, Taipei 106, Taiwan

*chumingwen@ntu.edu.tw

With the assistance of modern thin-film growth techniques, perovskite oxides with a three-dimensional crystal structure can now be grown in a layer-by-layer manner at atomic-level precision, opening up vast opportunities for unprecedented phenomena at the two-dimensional (2D) heterostructural interface. The emergence of a conductive interface between the two band insulators, LaAlO_3 (LAO) and SrTiO_3 (STO) [A. Ohtomo and H. Y. Hwang, *Nature* 427, 423 (2004)], represents the most celebrated exemplification in this framework. Up to the date, a plethora of oxide interfaces have been reported. It is, however, found that some of the interfaces remain insulating, whereas the same heterostructure-design concept as that of LAO/STO was exploited. To disentangle this puzzle, an atomic-scale spectroscopic characterization across the interfaces is indispensable and the quantitative chemical, electronic mapping by electron energy-loss spectroscopy (EELS) in conjunction with scanning transmission electron microscope (STEM) represents a powerful technique to this end. In this talk, I will explain the principles of atomically-resolved STEM-EELS and the unveiling of intriguing oxide-interfacial phenomena, ranging from the unexpected existence of a localized 2D electron density at the insulating $(\text{Nd,Sr})\text{MnO}_3/\text{STO}$ interface to the condensation of the 2D interfacial charges into one-dimensional electron chains by the misfit-dislocation strain field. The physics of the LAO/STO interface will be also scrutinized quantitatively with atomic accuracy.

New Developments for Material Physics in Electron Microscopy

Yukihito Kondo (近藤行人)*, Takaki Ishikawa (石川貴己), and Eiji Okunishi(奥西崇治)

EM Business unit JEOL Ltd., 3-1-2 Musashino Akishima Tokyo 196-8558 Japan

*kondo@jeol.co.jp

Development of modern microscope is accelerating, because the observation and analysis of an ultrafine structure are requested by semiconductor industry as well as materials physics. For the purpose, we have enhanced the resolution and analytical capabilities for 200 kV aberration corrected analytical microscope (JEM-ARM200F) by using a cold field emission gun, advanced aberration corrector and highly sensitive analytical system using multiple large solid angle silicon drift detectors (SDD).

The new cold field emission gun (CFEG) provides very high brightness ($>10^9$ A/(cm²*sr)), narrow energy spread (0.3 - 0.4 eV) in physical performance [1]. It also provides ease of use by procedure automation and good stability realized by ultimate vacuum condition around FE tip ($\sim 10^{-9}$ Pa). The new aberration corrector which correct 5th order aberration (including 6 fold astigmatism) is introduced to probe forming lens system. Together with narrow energy spread by CFEG, the microscope can form an atomic scale probe even if we use roughly double size of objective aperture with little affection of chromatic aberration. The new X-ray detection system employs double SDD, where each of detector have a sensing area of 100 mm². The total solid angle for the microscope is 1.7 sr. This high sensitivity enables us to perform analysis in shorter time and to detect trace element such as dopant in Si. Figure 1 shows atomic column elemental maps of SrTiO₃, obtained with the CFEG, the advanced corrector and the double detector analytical system. We can clearly see the separated atomic columns of Sr, Ti+O and O. We believe that the new analytical aberration corrected microscopes opens the innovations in cutting edge technologies.

Reference

1. Y Kohno *et al.*, *Microsc. Anal.* **24**, S9 (2010).

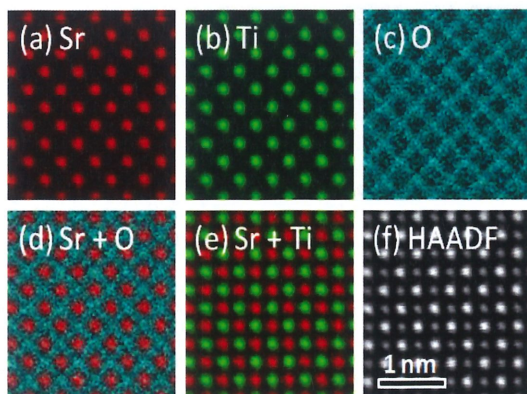


Figure 1. Elemental maps of SrTiO₃. (a) Sr, (b) Ti, (c) O, (d) Sr+O, (e) Sr+Ti, (f) HAADF STEM image.

Electron Microscopy 4.0: How Integrating Technologies Help Cure Diseases

Yong Yu (余涌)*

Life Science Unit, FEI

* yong.yu@fei.com

Electron microscopy has gone through a significant evolution the last few decades. From an elementary tool with an abundance of knobs and switches which required dedicated operators (EM 1.0) through development steps stabilizing the platforms, and increasing throughput (EM 2.0) it has arrived at the current situation (EM 3.0), a platform which is recognized for its ability to provide a complete and efficient workflow solution including sample preparation, imaging platforms, image acquisition, data output and data analysis.

Electron Microscopy 4.0 (EM 4.0) is the next step, and it is going to revolutionize microscopy both at the molecular and cellular level. In Cell biology the combination of various microscopy modalities, called correlative microscopy, will reveal cellular changes in-depth merging dynamics, labeling specificity and nanometer resolution - from a single experiment.

A similar evolution can be observed in the field of Structural Biology, which aim is to resolve protein structures at the molecular or atomic detail. Usually referred to as Integrated Structural Biology, the combination of XRD/NMR and Cryo-Electron Microscopy is quickly being adopted as the next step, gaining insight at the molecular level as the combination of these methods results in a continuum of scales and resolutions over a broad range, adding dynamics to the equation as well as the ability to study protein complexes rather than individual proteins only.

Electron microscopy 4.0, at all levels, will have a significant impact moving forward. The ability to combine technologies through dedicated workflow solutions will revolutionize biological research and will contribute significantly to curing disease.

Remodeling of Calcium Signaling in Tumor Progression

Meng-Ru Shen (沈孟儒)*

Department of Obstetrics & Gynecology, College of Medicine, National Cheng Kung University, Taiwan

* mrshen@mail.ncku.edu.tw

Intracellular calcium is an important signaling that modulates various cellular functions. The dysregulation of calcium homeostasis has been suggested as a critical event in driving the expression of the malignant phenotypes, such as proliferation, migration, invasion, and metastasis. Cell migration is an early prerequisite for tumor metastasis that has a significant impact on patient prognosis. During cell migration, the exquisite spatial and temporal organization of intracellular calcium provides a rapid and robust way for the selective activation of signaling components that play a central role in cytoskeletal reorganization, traction force generation, and focal adhesion dynamics. A number of known molecular components involved in calcium influx pathways, including stromal interaction molecule (STIM)/Orai-mediated store-operated calcium entry (SOCE) and the calcium-permeable transient receptor potential (TRP) channels, have been implicated in cancer cell migration and tumor metastasis. The clinical significance of these molecules, such as STIM proteins and the TRPM7 channel, in tumor progression and their diagnostic and prognostic potentials have also been demonstrated in specific cancer types. In this talk, I will summarize the recent advances in understanding the important roles and regulatory mechanisms of these calcium influx pathways on malignant behaviors of tumor cells. The clinical implications in facilitating current diagnostic and therapeutic procedures are also discussed.

Cell-to-cell Spread of Dengue Viruses

Chao-Fu Yang (楊朝富),¹ Cheng-Hsun Tu (杜承勳),¹ Ying-Ping Lo (羅尹萍)¹ Chih-Chieh Cheng (鄭至傑),¹ and Wei-June Chen (陳維鈞)^{1,2*}

¹Graduate Institute of Biomedical Sciences

²Department of Public Health and Parasitology, Chang Gung University, Kwei-San, Tao-Yuan, Taiwan

*wjchen@mail.cgu.edu.tw

The dengue virus (DENV), one of important arboviruses, is naturally transmitted by mosquitoes between humans. As a result, the DENV can easily infect cells derived from both hosts. Unlike in mammalian cells, however, the DENV usually causes extremely deleterious effects on cells of mosquitoes despite clustered progeny virions are usually formed within infected cells in a culture with high density of cells. It inspires us to think how the virus spreads between close-contact cells, particularly in those cells in tissues, *e.g.*, the midgut of mosquitoes. We observed that cell-to-cell spread is one way for the DENV to infect neighboring cells without depending on the mode of “release and entry”. Generally, a tetraspanin C189 upregulated in mosquito cells in response to the DENV infection may be incorporated to a membrane-bound vacuole within which newly formed DENV particles may exist. These virion-containing vacuoles are subsequently transported to the other cell, leading to intercellular transmission of the DENV from one cell to the other. Knockdown of C189 in DENV-infected C6/36 cells was shown to reduce the efficiency of cell-to-cell transmission which may be recovered by co-transfected with the C189-expressing vector in DENV-infected C6/36 cells. As cell-to-cell transmission was mostly occurred via the site of cell contact, it suggests that C189 is highly involved in intercellular spread of the viral particles from the infected donor cells to their directly contacted recipient cells. This novel finding is particularly worthwhile to account for rapid and efficient spread of the DENV in tissues with the mosquito.

References

1. C. C. Lin, C. F. Yang, C. H. Tu, C. G. Huang, Y. T. Shih, C. K. Chuang, and W. J. Chen. A novel tetraspanin C189 upregulated in C6/36 mosquito cells following dengue 2 virus infection. *Virus Res.* **124**, 176 (2007).
2. C. F. Yang, C. H. Tu, Y. P. Lo, C. C. Cheng, and W. J. Chen. Involvement of tetraspanin C189 in cell-to-cell spreading of the dengue virus in C6/36 cells. *PLoS Neglect. Trop. Dis.* (in press) (2015).

Nanoparticels for *in vitro* and *in vivo* Optical Imaging

Peilin Chen (陳培菱)*

Research Center for Applied Sciences, Academia Sinica, Taipei, Taiwan

*peilin@gate.sinica.edu.tw

In this talk, some recent developments in advanced imaging systems in our group will be discussed. We will first discuss the SERS spectroscopy from nanostructures and the confocal Raman imaging for SERS substrates. The same confocal Raman system can be used to image cells without labeling. Several nanoparticles such as quantum dots, gold nanoclusters and gold nanorods have been developed for bioimaging. By various surface functionalization schemes, it is possible to control the location of nanoparticles both *in vitro* and *in vivo* allowing the measurement of chemical environments inside cells and tumors.

The development of super-resolution microscopy, which has been used to monitor the distance between different proteins inside the focal adhesion as well as the density of protein, will be discussed in this talk. We have demonstrated that the force exerted by cells can be correlated with the density of proteins inside focal adhesions. The super-resolution microscopy has been extended to three-dimension allowing us to track the local pH value around the nanoparticles inside cancer cells. The acidification process of nanoparticles in the endocytosis process can be recorded. Such technique can be extended to detect the local chemical reaction inside living cells.

As for the tissue imaging, we have developed multi-photon microscopy using clearing reagent. It has been shown that blood vessels in the mouse whole brain can be imaged simultaneously. The penetration depth of multi-photon microscopy using clearing reagent can be deeper than 4 mm. On the same platform, it is possible to measure the movement of blood cells in living mouse at a frame rate higher than 100 frame/s. Such platform can also be used in imaging disease model and tumor samples from patients.

第三十五屆台灣顯微鏡學會學術演討會 學生論文壁報目錄

| 材料物理組 | | |
|-------|--|-------|
| MP-01 | Growth and Characterization of GaN Nanostructures Ko-Li Wu (吳可勵), Cheng-Chou Su (蘇誠洲), Chang-Hsun Huang (黃張勳), Chih-Meng Huang (黃智盟), Yi Chou (周易), Wei-I Lee (李威儀), and Yi-Chia Chou (周苡嘉) | p. 15 |
| MP-02 | The Effect of the Inhomogeneity in Individual Sides of FeSiBC Amorphous Ribbon on the Crystallization Behavior Po-Yu Chen (陳伯宇), Ya-Ling Chang (張雅齡), and Jer-Ren Yang (楊哲人) | p. 16 |
| MP-03 | Design and Application of In-situ TEM Holder with Thermal-electric Coupling Function Mu-Tung Chang (張睦東),* Shen-Chuan Lo (羅聖全), Ming-Wei Lai (賴明偉), Cheng-Yu Hsieh (謝承佑), and Ren-Fong Cai (蔡任豐) | p. 17 |
| MP-04 | Nanoindentation with Cross-Sectional TEM Analysis of the Deformation Behavior of Spinodal Nanostructured δ-ferrite in a 2205 Duplex Stainless Steel Yi-Chieh Hsieh (謝亦傑), Yu-Ting Tsai (蔡宇庭), and Jer-Ren Yang (楊哲人) | p. 18 |
| MP-05 | Effects of low-temperature asuforming on the microstructural evolution in Fe-0.6C-2Si-xMn (x=1, 2, wt%) nanobainitic steels Po-Yen Tung (童博彥), Yu-Ting Tsai (蔡宇庭), and Jer-Ren Yang(楊哲人) | p. 19 |
| MP-06 | Stability of Ge Nanowires and Metal Germinades Chih-Meng Huang (黃智盟), Pei-Wen Chen (陳佩玟), and Yi-Chia Chou (周苡嘉) | p. 20 |
| MP-07 | Effects of Nanometer-sized Interphase Precipitated Carbides on Deformation Behavior in Steels Chih-Hung Jen(鄭至閔), Shao-Pu Tsai (蔡邵璞), Yu-Ting Tsai (蔡宇庭), and Jer-Ren Yang (楊哲人) | p. 21 |
| MP-08 | The Coupling Behavior in Lenticular Martensite Y. L. Chang(張雅齡), P. Y. Chen (陳伯宇), S. W. Lai (賴世雯), and J. R. Yang (楊哲人) | p. 22 |
| MP-09 | The Effect of Mo in Niobium Contenting Low Carbon Steel Yu-Wen Chen (陳昱文), Bo-Ming Huang (黃柏銘) and Yu-Ting Tasi (蔡宇廷) | p. 24 |

| | | |
|-------|---|-------|
| MP-10 | Effect of Si on Interphase Precipitation Strengthened Dual-Phase Steels Shao-Pu Tsai (蔡劭璞), Cheng-Han Li (李承翰), Yuan-Tsuong Wang (王元聰), Ching-Yuan Huang (黃慶淵), and Jer-Ren Yang (楊哲人) | p. 25 |
| MP-11 | The Growth of χ Phase in SAF 2507 Duplex Stainless Steel Po-Chiang Lin (林帛江), Yi-Ling Tsai (蔡宇庭), Rudder Wu, Shing-Hoa Wang (王星豪), Jer-Ren Yang (楊哲人), and Hsueh-Ren Chen (陳學人) | p. 26 |
| MP-12 | Graphene Growth on γ Phase Aluminum Oxide Substrate Zhang-Cheng Luo (羅張誠), Chia-Hao Yu (余家濠), and Cheng-Yen Wen(溫政彥) | p. 27 |
| MP-13 | van der Waals Epitaxial Growth of Highly-textured ZnO Thin Film on the Surface-modified Silicon Substrate by Chemical Bath Deposition Chia-Hao Yu (余家濠), Kuan-Hung Chen (陳冠宏), Shao-Sian Li (李紹先), Zhang-Cheng Luo (羅張誠), Yi-Ren Zhang (張益仁), Chien-Ting Wu (吳建霆), Chun-Wei Chen (陳俊維), and Cheng-Yen Wen (溫政彥) | p. 28 |

| 生物醫學組 | | |
|-------|--|-------|
| BM-01 | Taxonomic Study of Piptocephalidaceae in Taiwan Chen-Ju Liu (劉貞汝) and Hsiao-Man Ho (何小曼) | p. 29 |
| BM-02 | The Ultrastructure of Microsymbionts in the Root Nodules of <i>Crotalaria Zanzibarica</i> Hsin-Mei Huang (黃心玫), Cheng-Tai Huang (黃承泰), and Shiang-Jiuun Chen (陳香君) | p. 30 |

Growth and Characterization of GaN Nanostructures

Ko-Li Wu (吳可勵), Cheng-Chou Su (蘇誠洲), Chang-Hsun Huang (黃張勳), Chih-Meng Huang (黃智盟), Yi Chou (周易), Wei-I Lee (李威儀), Yi-Chia Chou (周苡嘉)*

Department of Electrophysics, National Chiao Tung University, Hsinchu, Taiwan

*ycchou@nctu.edu.tw

GaN is a popular material since last decade because of the wide and direct band gap which benefits to a variety of applications such as visible and UV optoelectronics, and high-power high-temperature and high-frequency electronic devices. GaN-on-Si has attracted considerable attentions recently and it is believed to dominate the GaN power electronics market in next generation semiconductor industry. Considering the lattice mismatches, the substrate selection is critical for the quality of GaN crystal growth. Here we have investigated one-dimensional GaN nanostructures grown on three different types of substrates, Si(111), Si(100) and sapphire, by hydride vapor phase epitaxy (HVPE) using the catalyst-assisted process. Metals were deposited on the substrates by electron gun evaporation which serve as catalysts and the GaN nanostructures were then grown by vapor-liquid-solid mechanism. The morphology, crystallography and structures investigated by X-ray diffraction and scanning electron microscopy will be discussed.

The Effect of the Inhomogeneity in Individual Sides of FeSiBC Amorphous Ribbon on the Crystallization Behavior

Po-Yu Chen (陳伯宇),* Ya-Ling Chang (張雅齡), and Jer-Ren Yang (楊哲人)

Department of Materials Science and Engineering, National Taiwan University, Taipei, Taiwan

*d00527002@ntu.edu.tw

This work focuses on the analysis of crystallization behavior in annealed FeSiBC amorphous ribbon. The ribbon produced by melt-spinning method is significantly influenced by the manufacturing process and has different surface morphology in its individual sides: shiny side for contacting air, and matt side for contacting wheel. Such a discrepancy in morphology also means that there exists different strain energy in individual sides and brings out different crystallization behaviors. In this FeSiBC amorphous ribbon, dendritic crystal (α -Fe) is the main product after annealing treatment. The growth direction of dendritic crystal is essential for this investigation and observed with transmission electron microscopy (TEM). From x-ray diffraction and electron backscatter diffraction (EBSD) analysis, it indicates that after heat treatment below 470°C, α -Fe crystallites on the shiny side are oriented little preferentially parallel to (1 0 0) direction, while those on the matte side are not. However, treatment at higher temperature drives this discrepancy to decrease. It is therefore to conclude that the strain causes the different preferred texture of α -Fe crystallites in respective sides and the new transformation product Fe₂B at higher annealing temperature inhibits this tendency.



Figure 1. EBSD analysis of cross-section of annealed FeSiBC amorphous ribbon. The sample was heat treated at 450°C for 60 min.

Design and Application of In-situ TEM Holder with Thermal-electric Coupling Function

Mu-Tung Chang (張睦東),* Shen-Chuan Lo (羅聖全),Ming-Wei Lai (賴明偉)
Cheng-Yu Hsieh (謝承佑) and Ren-Fong Cai (蔡任豐)

Department of Electron Microscopy Development and Application, Material and Chemical Research Laboratories, Industrial Technology Research Institute (ITRI)

* mtchang@itri.org.tw

In-situ Transmission Electron Microscope (TEM) with heating and biasing coupling platform is a powerful technique for driven-reaction mechanism study of energy industry with spatial resolution down to atomic scale. In this study, we develop the design and application of in-situ TEM holder with thermal-electric coupling function. The piezo-driven technique and modified heater are integrated in this design. It is very similar to real environment in Li-based battery. In addition, the combination of in-situ TEM/STEM image and EDS/EELS analysis represents a helpful tool to link the physical and chemical structure of observed target to their macroscopic properties. The achievements of this study will be adopted by ITRI as the technical base for future analysis works which are related to in-situ TEM observations. The design and application of in-situ TEM holder with multi-functional platform is to establish advanced electron microscopy analysis techniques for unknown mechanism study.

References

1. H. Y. Wua *et al.*, *Electrochim. Acta* **138**, 30, (2014).
2. D. Saikia *et al.*, *J. Power Sources* **269**, 651, (2014).
3. X. Tian *et al.*, *Nano Res.* s12274, (2014).
4. R. Xu *et al.*, *ACS Appl. Mater. Inter.* (2014).

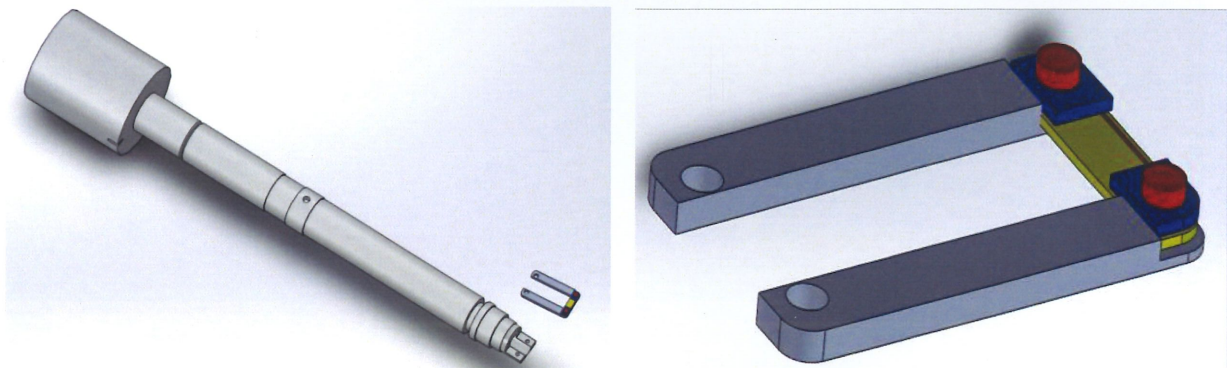


Figure 1. Scheme of in-situ holder with thermal-electric coupling function.

Nanoindentation with Cross-Sectional TEM Analysis of the Deformation Behavior of Spinodal Nanostructured δ -ferrite in a 2205 Duplex Stainless Steel

Yi-Chieh Hsieh (謝亦傑),* Yu-Ting Tsai (蔡宇庭), and Jer-Ren Yang (楊哲人)

Department of Materials Science and Engineering, National Taiwan University, Taipei, Taiwan

*r02527001@ntu.edu.tw

The nanoindentation with cross-sectional TEM analysis was carried out to investigate the interaction between dislocations and the spinodal structure (as shown in Fig. 1) in 2205 duplex stainless steels, which were either unaged or aged at 475°C for 64h. The effects of the spinodal structure including limitations of the deformation ability and cross-slip were observed in the aged δ -ferrite film. In the moderate strain area, the spinodal structure resulted in the cross-stitch pattern and slip bands in the aged δ -ferrite film. In the high strain area, the dislocations close to the nanoindent were confined by the spinodal structure and early formed dislocations together, resulting in the serious lattice distortion and curved dislocation morphology in the aged δ -ferrite film.

References

1. K. L. Weng, H.R. Chen, and J. R. Yang, *Mater. Sci. Eng. A* **379**, 119 (2004).
2. L. Zhang and T. Ohmura, *Phys. Rev. Lett.* **112**, 145504 (2014).

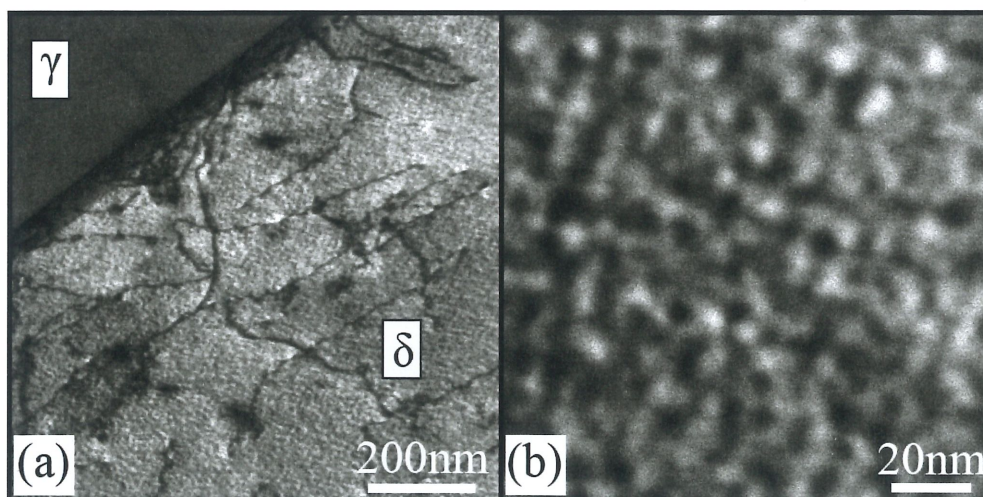


Figure 1. TEM bright field images of the aged specimen: (a) Around the δ/γ interface; (b) Modulated contrast of the spinodal structure.

Effects of Low-temperature Ausforming on the Microstructural Evolution in Fe-0.6C-2Si-xMn (x=1, 2, wt%) Nanobainitic Steels

Po-Yen Tung (童博彥), Yu-Ting Tsai (蔡宇庭), and Jer-Ren Yang(楊哲人)*

Department of Materials Science and Engineering, National Taiwan University, Taipei, Taiwan

*jryang@ntu.edu.tw

Nanostructured bainite [1], having high potential as the bulletproofing material, has been studied for many years. Nanostructured bainite possesses high strength, high elongation, but its low toughness due to the instability of blocky austenite is a serious disadvantage. So, the primary propose in this work is to improve the properties of blocky austenite. First, we introduce ausforming process—plastic deformation at low temperature before isothermal bainitic transformation—to change the microstructure of traditional nanostructured bainite. Second, we further measure the stability of blocky austenite in ausformed bainite by EBSD. Besides, the orientation relationship between blocky austenite and bainitic ferrite is analyzed by EBSD. In ausformed bainite, the blocky austenite and bainitic sheaves are simultaneously refined and well-distributed. The refined blocky austenite is further mechanical stabilized by ausforming process, which might benefit to mechanical properties. Due to ausforming process, variant selection is assisted by Shockley partial dislocations and measured by EBSD.

Reference

1. F. G. Caballero, H. Bhadeshia, K. J. A. Mawella, D. G. Jones, and P. Brown, *Mater. Sci. Technol.* **18**, 279 (2002).

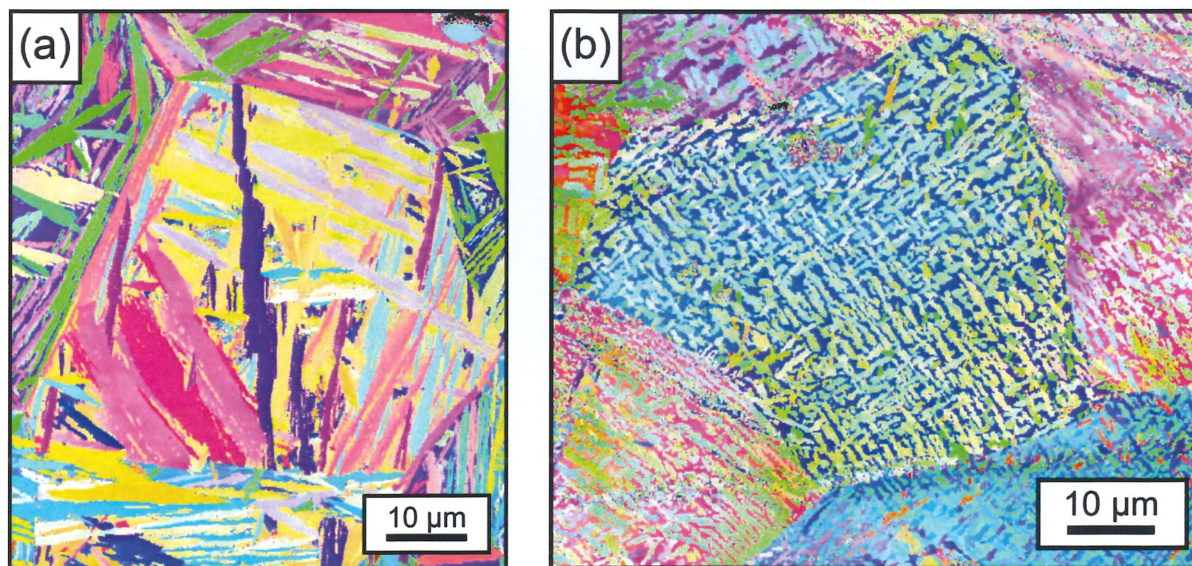


Figure 1. Inverse pole figure (IPF) map of (a) non-ausformed specimen with random growth of bainite; (b) ausformed specimen with bainitic variant selection.

Stability of Ge Nanowires and Metal Germanides

Chih-Meng Huang (黃智盟), Pei-Wen Chen (陳佩玟), Yi-Chia Chou (周苙嘉)*

Department of Electrophysics, National Chiao Tung University, Hisnchu City 300, Taiwan

*ycchou@nctu.edu.tw

Following the advances of semiconductor nano-technology, the size of electronic transistors and components become smaller and smaller. Therefore, one dimensional nanostructures such as nanowire attract attention for the development of next generation devices. Current semiconductor transistors are mainly Si-based due to the stable and reliable electronic properties of Si; however, Ge has recently been considered again for the development of building blocks due to its higher carrier mobility than that of Si and the significant progress in technology of high-k dielectric materials. It requires more systematic studies for Ge system regarding the stability of the native oxide to proceed further to the real industrial use.

We have investigated the reactions of Ge nanowires, with and without oxide, and Ni nanoparticles by annealing at different temperatures. Ge nanowires were grown by vapor-liquid-solid mechanism. The buffered hydrofluoric acid steam was used to etch the native oxide or oxide shell on Ge nanowires. Thin Ni films were deposited on the samples by the electron beam evaporation. The annealing temperature ranges between 300~500 °C with the ramping rate of 1 °C/s in a furnace. The surface morphology and characterizations of Ge nanowires and NiGe in nanowires were studied using SEM, TEM, and EDS.

Effects of Nanometer-sized Interphase Precipitated Carbides on Deformation Behavior in Steels

Chih-Hung Jen(鄭至閔),* Shao-Pu Tsai (蔡邵璞), Yu-Ting Tsai (蔡宇庭),
and Jer-Ren Yang (楊哲人)

Department of Materials Science and Engineering, National Taiwan University, Taipei,
Taiwan

*tabonster@gmail.com

The interphase precipitation has been considered a potential strengthening mechanism for ferrite phase in recent ten years. Although many research results had confirmed and valued the contribution of interphase precipitation, few efforts are laid on understanding the effects on deformation behaviors [1]. And the analysis of dislocation microstructures was limited due to the distortion from deformation [2]. In the present work, annular dark field (ADF) imaging in scanning transmission electron microscopy (STEM) was adopted to obtain the clear image of dislocation microstructure in the deformation process. Interphase precipitation can serve an additional source of dislocation multiplication. And with interphase precipitation, the dislocation microstructures inside the ferrite grain developed much more homogeneously. Evolution of dislocation microstructures can be correlated to the deformation behavior successfully.

References

1. N. Kamikawa, Y. Abe, G. Miyamoto, Y. Funakawa, and T. Furuhashi, *ISIJ Int.* **54**, 212 (2014).
2. E. V. Nesterova, S. Bouvier, and B. Bacroix, *Mater. Charact.* **100**, 152 (2015).

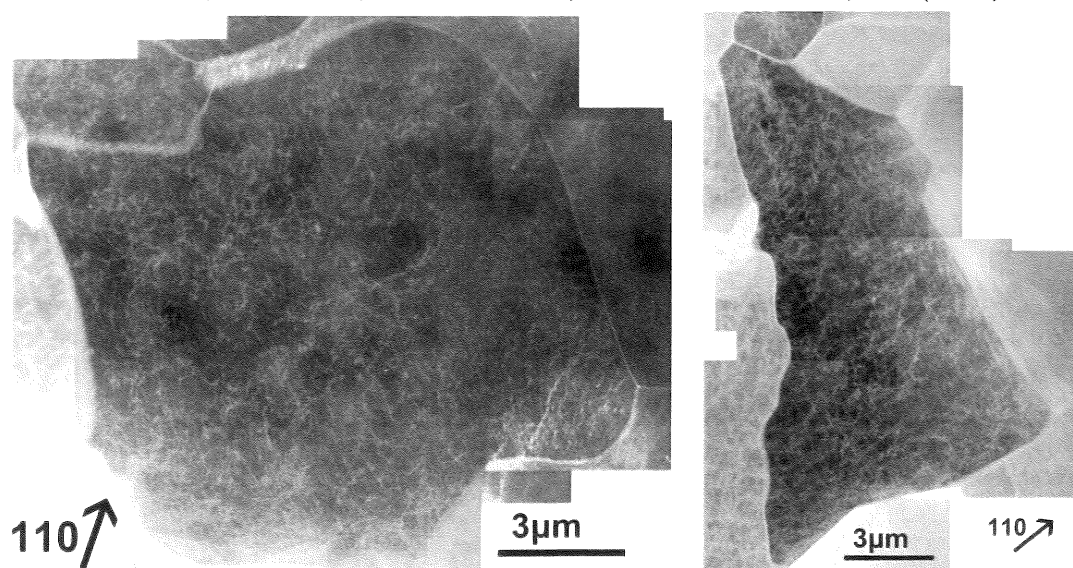


Figure 1. STEM ADF of ferrite grain without interphase precipitation subjected to 0.75% strain.

The Coupling Behavior in Lenticular Martensite

Y. L. Chang (張雅齡)*, P. Y. Chen (陳伯宇), S. W. Lai (賴世雯), and J. R. Yang (楊哲人)

Department of Materials Science and Engineering, National Taiwan University, Taipei, Taiwan

*d99527007@ntu.edu.tw

This research focuses on the micro- and macro-structure of lenticular martensite in AISI 440C stainless steel. At first, EBSD is used to investigate the crystal orientation relationship in lenticular martensite. The techniques can provide the information of crystal orientation in different aspects and attain more details in the crystallography. The ideal condition for analyzing the orientation of martensite units is based on large enough prior austenite grain size which can avoid the impingement between each lenticular martensite grain. The growing arrangement and coupling of lenticular martensite was then investigated. The results showed that the variant pairs between each lenticular martensite grains tend to be 1V-6V, 1V-16V and 1V-17V. Therefore, the orientation relationship between lenticular martensite and austenite matrix in this high-C high-Cr alloying steel is precisely confirmed as Kurdjumov-Sachs (K-S) orientation relationship.

References

1. A. Shibata, S. Morito, and T. Furuhashi, *et al.*, *Scr. Mater.* **53**, 597 (2005).
2. A. Stormvinter, P. Hedstrom, and A. Borgenstam, *J. Mater. Sci. & Technol.* **29**, 373 (2013).
3. H. Okamoto, M. Oka, and I. Tamura, *Trans. JIM* **19**, 674 (1978).

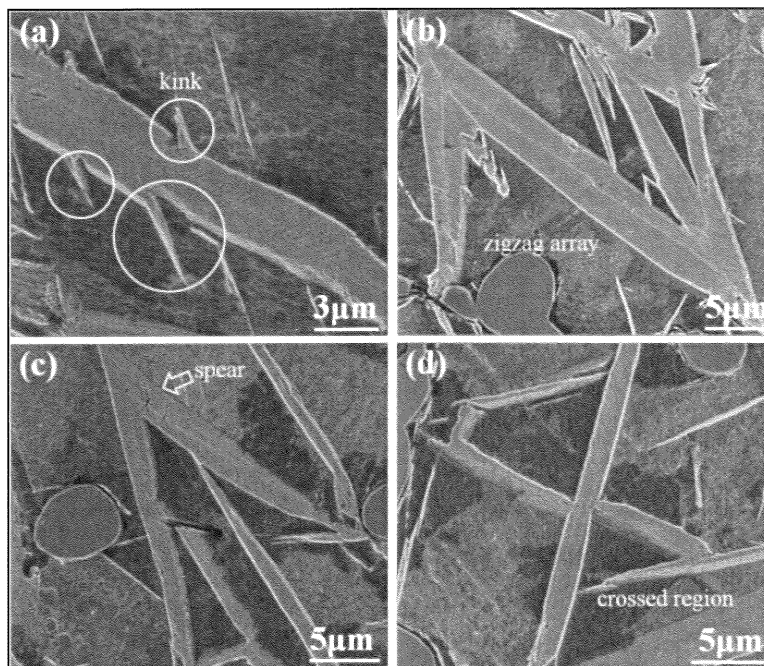


Figure 1. SEM images showing the (a) kink, (b) zigzag array, (c) spear, and (d) crossed region morphology of lenticular martensite

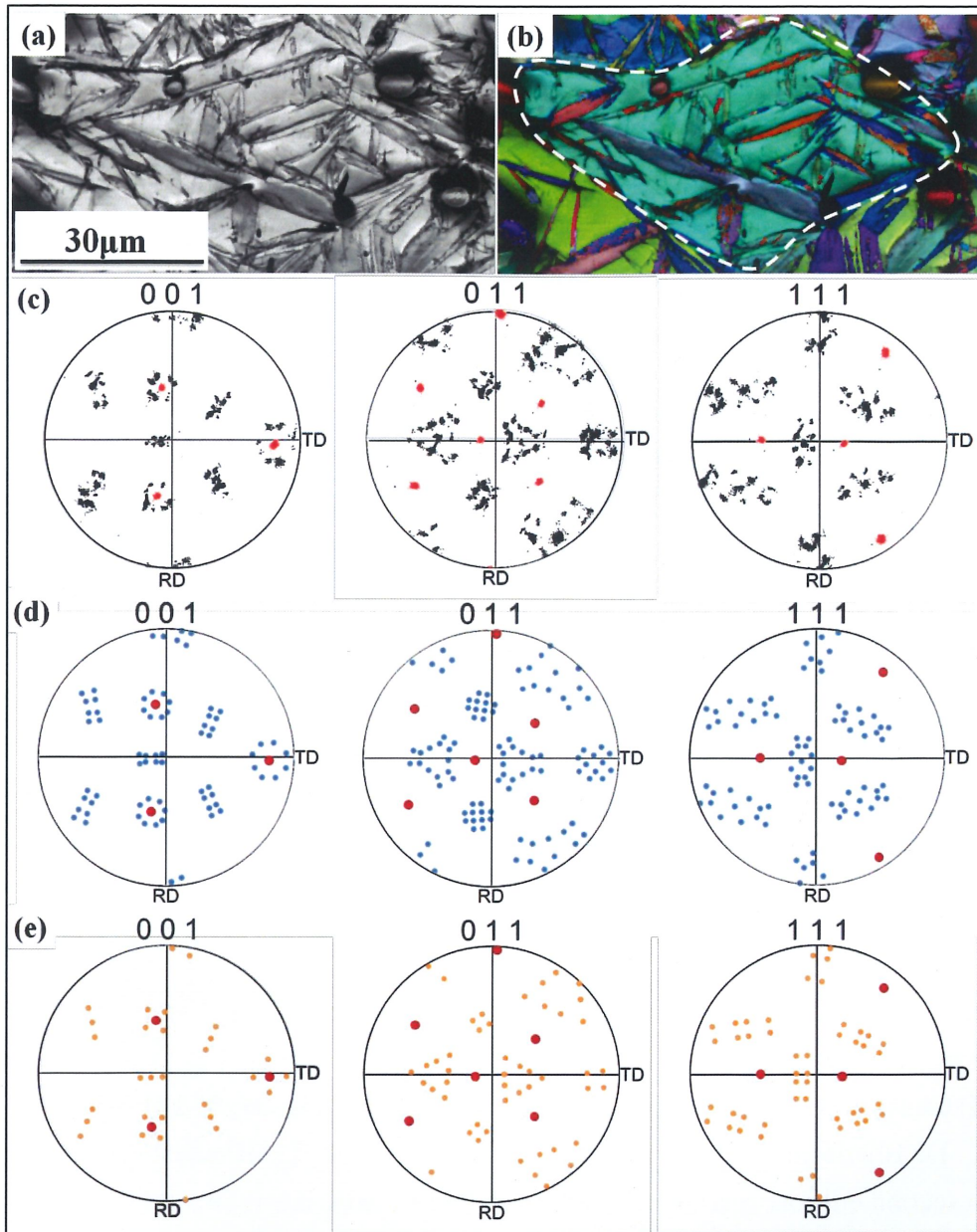


Figure 2. (a) Image quality (IQ) map; (b) Inverse pole figure (IPF) colored map; (c) $\{100\}$, $\{110\}$, $\{111\}$ pole figure of experimental results; (d) $\{100\}$, $\{110\}$, $\{111\}$ pole figure of simulated K-S OR; (e) $\{100\}$, $\{110\}$, $\{111\}$ pole figure of simulated N-W OR.

The Effect of Mo in Niobium Contenting Low Carbon Steel

Yu-Wen Chen (陳昱文),* Bo-Ming Huang (黃柏銘), and Yu-Ting Tasi (蔡宇廷)

Department of Materials Science and Engineering, National Taiwan University, Taipei, Taiwan

*f01527051@ntu.edu.tw

In the present research, the secondary hardening effects of Nb-containing strips with and without Mo addition were investigated. Hardness results show that with 0.3 wt% Mo addition, the significant secondary hardening occurred after 10 minutes tempering at 700°C, and the hardness was maintained even after severing tempering. In contrast, the hardness only showed minor secondary hardening for strips without Mo addition. The effects of Mo on Nb-containing strips during 700°C tempering were investigated with scanning electron microscope, electron backscattered diffraction and transmission electron microscope. Quantitative metallography results showed that the phase fractions of ferrite, bainite and second phase did not change, but coalescence did occur in bainite, regardless of Mo addition. Molybdenum had the effects of maintaining carbide size, and together with increased M/A constituent, resulted in significant secondary hardening effect.

References

1. J. R. Yang, C.Y. Huang, C.S. Chiou, *ISIJ Int.* **35**, 1013 (1995).
2. B. M. Huang, J. R. Yang, H.W. Yen, C.H. Hsu, C.Y. Huang, H. Mohrbacher, *Mater. Sci. Technol.* **30**, 1014 (2014).
3. C. Y. Huang, J. R. Yang, and S. C. Wang, *Mater. Tran. JIM*, **34**, 658 (1993).
4. H. K. D. Bhadeshia, Mechanical Properties, in: H. K. D. Bhadeshia (Ed.) *Bainite in steels* second edition, Institute of Materials, 285 (2001).

Effect of Si on Interphase Precipitation Strengthened Dual-Phase Steels

Shao-Pu Tsai (蔡劭璞),¹ Cheng-Han Li (李承翰),¹ Yuan-Tsuong Wang (王元聰),²
Ching-Yuan Huang (黃慶淵),² and Jer-Ren Yang (楊哲人)^{1*}

¹Department of Materials Science and Engineering, National Taiwan University, Taipei, Taiwan

²Department of Research and Development, China Steel Corporation, Kaohsiung, Taiwan

*jryang@ntu.edu.tw

Si is shown to promote ferrite transformation rate in this study. In all temperature ranges of two phase region, the higher the Si addition, the higher the ferrite volume fraction, which results from the characteristic that Si is α -stabilizer. The character as α -stabilizer of Si is also proven by determination of Ac1 and Ac3 by dilatometer curve. Si is proven to have the effect of solid solution strengthening [1, 2], while the hardness data show that if Ti is added, the hardness difference will either remain the same or be slightly degraded, where in the latter case, strengthening comes both from Si solid solution strengthening and TiC interphase precipitation strengthening. TEM investigation of interphase precipitation indicate as Si is added, both sheet spacing and intercarbide spacing will increase under the same temperature, which is thought to be the main reason that strength difference will be the same or slightly lower than strength difference of steels only different in Si content. Strength contribution of interphase precipitation is also estimated using equation from [3].

References

1. T Gladman. The physical metallurgy of microalloyed steels. Institute of Materials. London (1997).
2. R. G. Davies, *Metall. Trans. A* **10**,113 (1979).
3. H. W. Yen, P. Y. Chen, C. Y. Huang, and J. R. Yang, *Acta Mater.* **59**, 6264 (2011).

The Growth of χ Phase in SAF 2507 Duplex Stainless Steel

Po-Chiang Lin (林帛江),^{1*} Yi-Ling Tsai (蔡宇庭),² Rudder Wu,³

Shing-Hoa Wang (王星豪),¹ Jer-Ren Yang (楊哲人),² Hsueh-Ren Chen (陳學人)²

¹Department of Mechanical and Mechatronic Engineering, National Taiwan Ocean University, Keelung 20224, Taiwan

²Department of Materials Science and Engineering, National Taiwan University, Taipei, Taiwan

³Research Center for Strategic Materials, National Institute for Materials Science, Japan

*j2034457@hotmail.com.tw

Duplex stainless steel of SAF 2507 was exposed at 600°C for 7 hours under aging condition. It was found that the χ phase transformed inside the ferritic grain which agreed with the literature reports [1, 2]. The formation of χ phase nucleated at the dislocation in α matrix initially under aging at 600°C for 7 hours. Then they grew into either the needle plates along one direction or the mutual perpendicular needle plates along two orientations. The dislocation loops formed around the mutual perpendicular needle plates might be brought on by the misfit strain between α matrix and the needle plate of χ phases (Fig. 1). The neat microstructure of a blocky χ phase was characterized by many stacked thin plates observed under enlarged high magnification as aging at 750 °C for 5 hours.

References

1. J. K. Du, C. H. Wang, K. C. Wang, and K. K. Chen, *Intermetallics* **45**, 80 (2014),
2. A. Kashiwar, N. Phani Vennela, S.L. Kamath, and R. K. Khatirkar, *Mater. Charact.* **74**, 55 (2012).

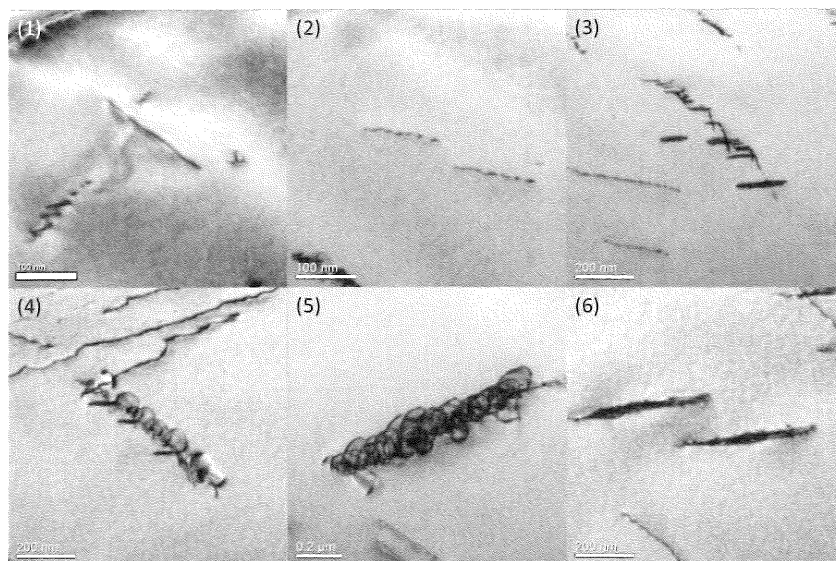


Figure 1. The sequence of χ phase growth at 600°C for 7hours.

Graphene Growth on the γ Phase Aluminum Oxide Substrate

Zhang-Cheng Luo (羅張誠), Chia-Hao Yu (余家濠), and Cheng-Yen Wen(溫政彥)*

Department of Materials Science and Engineering, National Taiwan University, Taipei, Taiwan

*cwen@ntu.edu.tw

Al_2O_3 is a good dielectric material and the dielectric constant is larger than SiO_2 so that it is useful for future VLSI device application. In addition, recent research found that sapphire can catalyze graphene growth in methane at temperature higher than 1100°C . In order to decrease the growth temperature, we try to change the carbon source and the phase of Al_2O_3 in the growth experiments. We find that $\gamma\text{-Al}_2\text{O}_3$ can catalyze graphene growth without hydrogen with the use of acetylene as the carbon source. We use transmission electron microscopy (TEM) and scanning electron microscopy (SEM) to characterize the morphology and interfacial properties of the graphene layers grown on the dielectric substrates. Raman spectroscopy and electrical measurements are used to certify their quality. The TEM cross-sectional image in Fig. 1(a) shows that graphene layers are grown on the $\gamma\text{-Al}_2\text{O}_3$ surface. The Raman spectrum in Fig. 1(b) shows the 2D band indicating the formation of graphene layers. However, under low temperature condition, the carbon precursors are only decomposed and adsorbed on the $\gamma\text{-Al}_2\text{O}_3$ surface, without the formation of graphene layers.

References

1. K. I. Bolotin, K. J. Sikes, Z. Jiang, M. Klima, G. Fudenberg, J. Hone, P. Kim, and H. L. Stormer, *Solid State Commun.* **146**, 351 (2008).
2. J. Kang, D. Shin, S. Bae, and B. H. Hong, *Nanoscale* **4**, 5527 (2012).

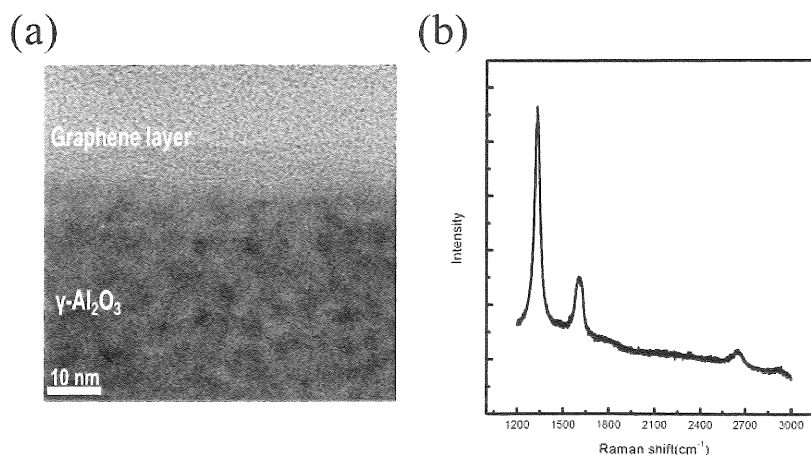


Figure 1. Cross-sectional TEM image and Raman spectrum of the graphene film grown on $\gamma\text{-Al}_2\text{O}_3$.

van der Waals Epitaxial Growth of Highly-textured ZnO Thin Film on the Surface-modified Silicon Substrate by Chemical Bath Deposition

Chia-Hao Yu (余家濠),¹ Kuan-Hung Chen (陳冠宏),¹ Shao-Sian Li (李紹先),¹ Zhang-Cheng Luo (羅張誠),¹ Yi-Ren Zhang (張益仁),¹ Chien-Ting Wu (吳建霆),² Chun-Wei Chen (陳俊維),¹ and Cheng-Yen Wen (溫政彥)^{1*}

¹Department of Materials Science and Engineering, National Taiwan University, Taipei, Taiwan

²National Nano Device Laboratories, National Applied Research Laboratories, Hsinchu City, Taiwan

*cwen@ntu.edu.tw

Zinc oxide is a multifunctional material with excellent properties for optical, optoelectronic, and piezoelectric applications. One of the routinely used methods of ZnO nanostructure growth is chemical bath deposition (CBD), which is a low-cost and straightforward process for large-area fabrication. In order to control the growth direction of ZnO nanorods, we modify the surface structure of silicon substrates using the self-assembly monolayer (SAM) method. Without the use of SAM, ZnO nanorods are randomly grown on the SiO₂ substrate (Fig. 1(a)). Highly-textured ZnO rods can form on both APTMS- and OTMS-modified substrates (Fig. 1(b) and Fig. 1(c-d), respectively). From the X-ray diffraction (XRD) and photoluminescence (PL) analysis results, we find that the ZnO thin film grown on silicon surface ended with the methyl group is highly c-axis oriented. We use transmission electron microscopy (TEM) for further studying the structure of the coalesced ZnO nanorods.

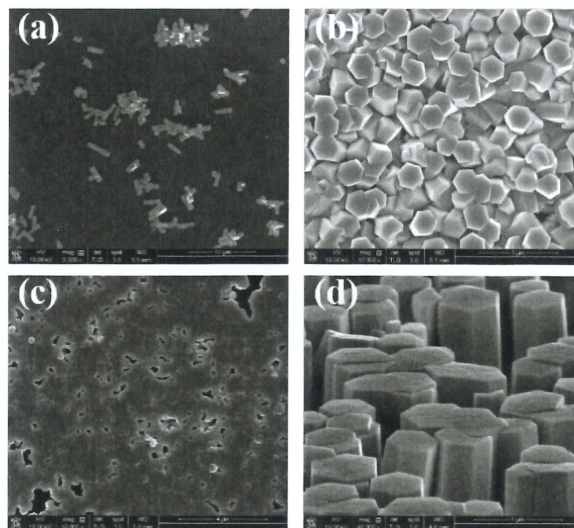


Figure 1. SEM images of ZnO grown by CBD on (a) pure SiO₂ substrates; (b) APTMS-modified substrates; (c) OTMS-modified substrates; (d) OTMS-modified substrates in an inclined viewing direction.

Taxonomic Study of Piptocephalidaceae in Taiwan

Chen-Ju Liu (劉貞汝) and Hsiao-Man Ho (何小曼)*

Department of Science Education, National Taipei University of Education, Taipei, Taiwan

*ho@tea.ntue.edu.tw

Members of Piptocephalidaceae (Zoopagales, Zoopagomycotina) are obligate mycoparasites, mostly grow on Mucorales, which are usually isolated from soil or dung of herbivores and small rodents. The family now comprises three genera, *Piptocephalis*, *Kuzuhaea* and *Syncephalis*. The distinctive morphological characters of Piptocephalidaceae are hyaline, delicate, septate or non-septate vegetative hyphae; simple or branched, septate or non-septate sporangiophore; cylindrical merosporangia born on terminal deciduous or nondeciduous enlargement and sporangiospores usually uniseriate.

In this study, 1271 soil and 120 dung samples were collected from countrysides, forests, houses, national parks and arboretums in Taiwan. There were 34 Piptocephalidaceous strains isolated. Based on morphological character, eleven species which are *Piptocephalis freseniana*, *Syncephalis cornu*, *S. depressa*, *S. obliqua*, *S. intermedia*, *S. sphaerica*, *S. tenuis*, *S. vivipara* and three new *Syncephalis* species were identified. Among them, *S. intermedia* is new records to Taiwan. Morphological characters were illustrated and described.

References

1. R. K. Benjamin, The merosporangiferous Mucorales. *Aliso* **4**, 321 (1959).
2. T. Gräfenhan, Taxonomic revision of the genus *Piptocephalis* (Fungi). Master's thesis. Mathematisch-Naturwissenschaftlichen Fakultät der Ernst-Moritz-Arndt-Universität Greifswald, Germany (1998).
3. H. M. Ho and G. L. Benny, Two new species from Taiwan, with a key to the *Syncephalis* species found in Taiwan. *Bot. Stud.* **48**, 319 (2007).
4. H. M. Ho and G. L. Benny, A new species of *Syncephalis* from Taiwan. *Bot. Stud.* **49**, 45 (2008).

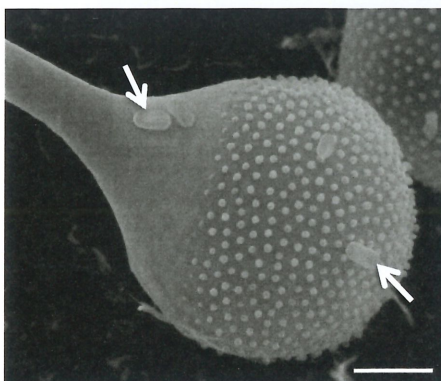


Figure 1. *Syncephalis obliqua*. Head cell with merospores (arrows). Bar = 10 μm .

The Ultrastructure of Microsymbionts in the Root Nodules of *Crotalaria Zanzibarica*

Hsin-Mei Huang (黃心玫),¹ Cheng-Tai Huang (黃承泰),² and Shiang-Jiuun Chen (陳香君)^{3*}

¹Department of Biochemical Science and Technology, National Taiwan University

²Institute of Ecology and Evolutionary Biology, National Taiwan University

³Department of Life Science, National Taiwan University

*hjchen@ntu.edu.tw

Legumes (Family Fabaceae) commonly establish symbiosis with rhizobia, forming N₂-fixing nodules on roots. In the nodules, rhizobia are wrapped inside symbiosome and differentiate into N₂-fixing bacteroids [1]. In this study, we analyzed root nodules of *Crotalaria zanzibarica*, a widespread naturalized legume in Taiwan. Genus *Crotalaria* is phylogenetically distant from other model legumes. Correspondingly, we showed that the symbiotic traits of *C. zanzibarica* differed from that of any known model legumes, indicating diverse mechanisms underlie legumes-rhizobia symbiosis [2].

References

5. K. M. Jones, H. Kobayashi, B. W. Davies, M. E. Taga, and G. C. Walker, *Nat Rev Microbiol.* **5**, 619 (2007).
6. R. Oono, I. Schmitt, J. I. Sprent, and R. F. Denison, *New Phytol.* **187**, 508 (2010).

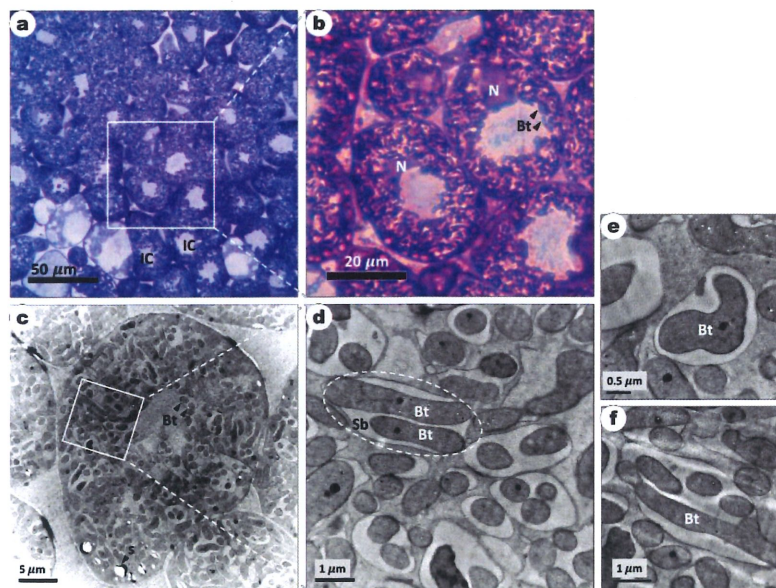
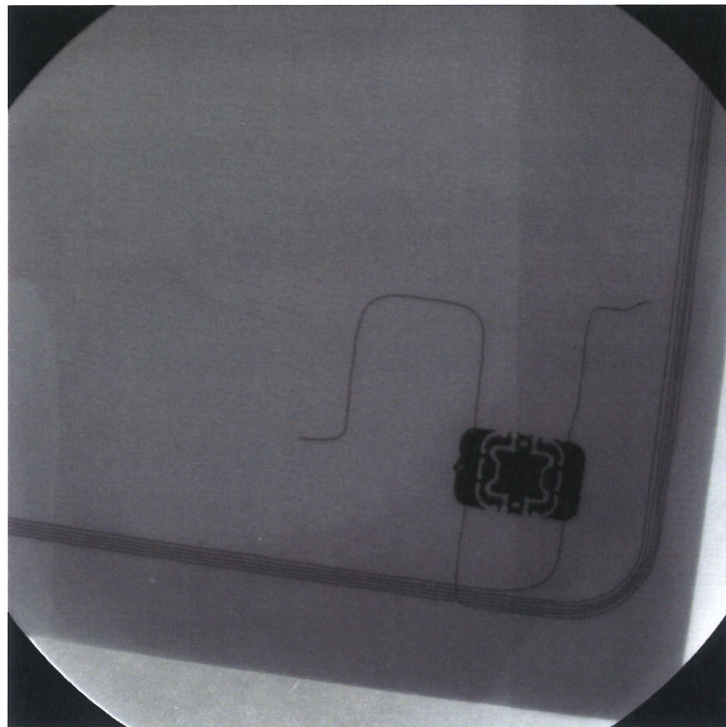


Figure 1. Longitudinal sections of root nodule of *C. zanzibarica* showed side-by-side distribution of infected cells. Infected cells were packed with darkly-stained bacteroids except for central region (a & b). Starch grains scattered on the periphery. In general, each symbiosome harbored multiple bacteroids (c). Bacteroids were elongated (d), swollen (e), or branched (f). IC: infected cell; N: nucleus; Bt: bacteroid; S: starch grain; Sb: symbiosome.

第三十五屆台灣顯微鏡學會學術演討會 顯微攝影作品目錄

| | | |
|------|---|-------|
| P-01 | 我的 RFID 李志浩 國立清華大學工程與系統科學系 | p. 32 |
| P-02 | 星空下的天燈 蘇誠洲、吳可勵、周易、黃智盟 國立交通大學物理所 | p. 33 |
| P-03 | 奈米侏儸紀 暴龍的入侵 謝亦傑 國立台灣大學材料科學與工程學系 | p. 34 |
| P-04 | 火鳳神鷹 童博彥 國立台灣大學材料科學與工程學系 | p. 35 |
| P-05 | 在黑色的大海中竄上的鮪魚 鄭至閔 國立台灣大學材料科學與工程學系 | p. 36 |
| P-06 | 腦漿中白色寄生蟲 廖敏任 國立台灣海洋大學機械與機電所 | p. 37 |
| P-07 | 皇宮中的旋轉樓梯 陳昱文 國立台灣大學材料科學與工程學系 | p. 38 |
| P-08 | 久旱不雨，稻田龜裂 林帛江 國立臺灣海洋大學機械與機電所 | p. 39 |
| P-09 | 太空天梯 蔡劭璞 國立台灣大學材料科學與工程學系 | p. 40 |
| P-10 | 派大星星知我心 簡亨達、李婉綺、康敦彥 國立台灣大學化學工程學系 | p. 41 |
| P-11 | 隱藏版美食—梅花糕 李紹輔 中興大學生命科學系 | p. 42 |
| P-12 | 蓮花出淤泥而不染 王惇平、李婉綺、康敦彥 國立臺灣大學化學工程學系 | p. 43 |



作品名稱：我的 RFID

作品內容

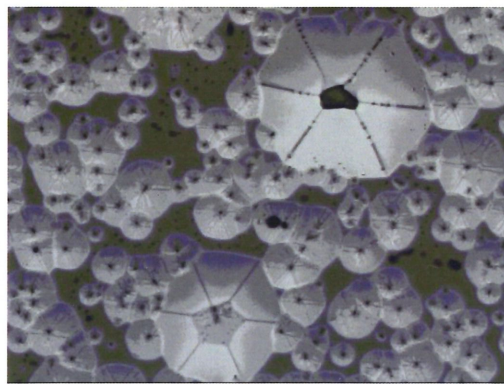
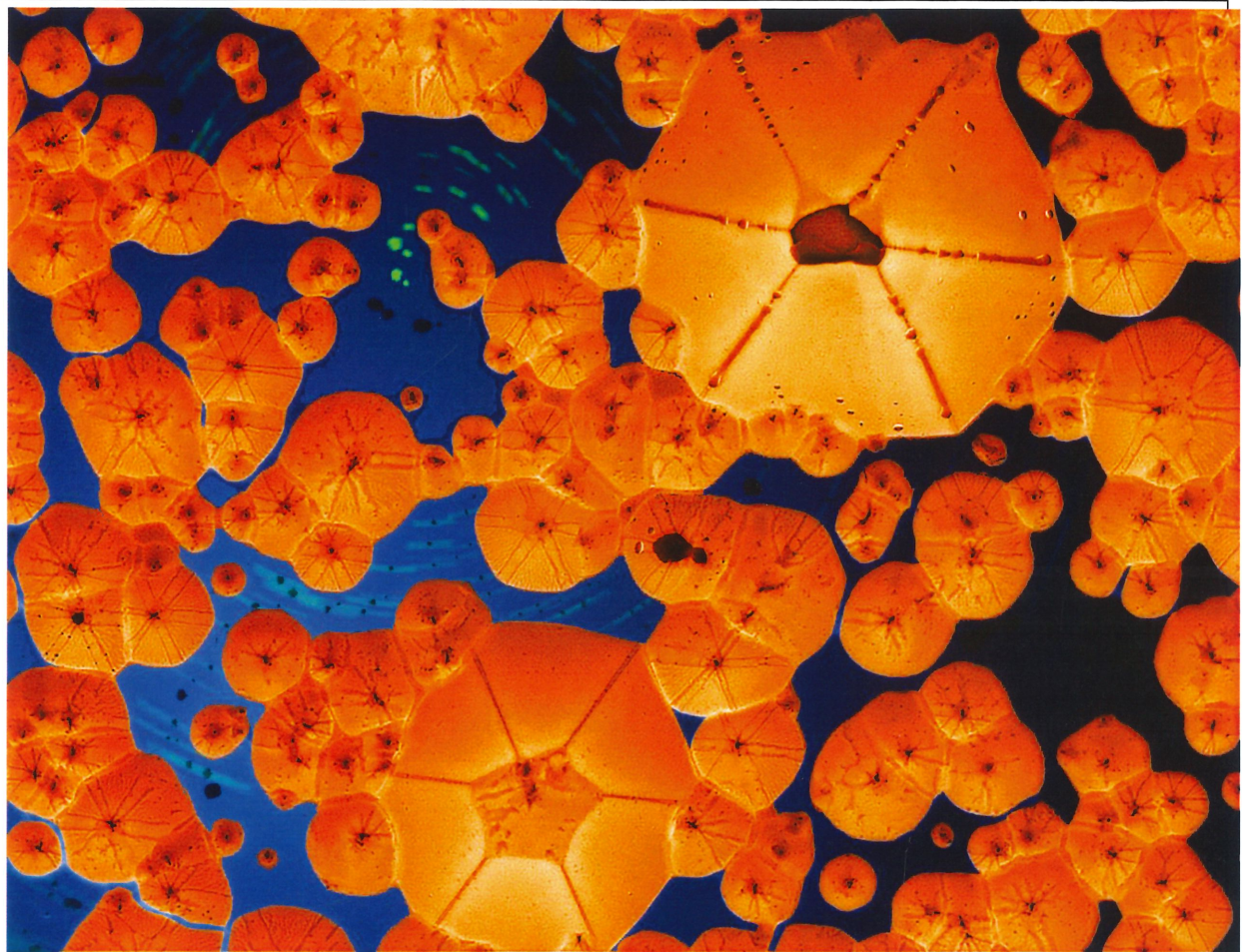
我的服務證以微聚焦 X 光機與 X 光 CCD 成像，倍數 x10。RFID 還有天線，XRF 證實為銅線。

作者姓名：李志浩

學校單位：

國立清華大學工程與系統科學系

E-Mail：chlee@mx.nthu.edu.tw



作品名稱：星空下的天燈

作品內容

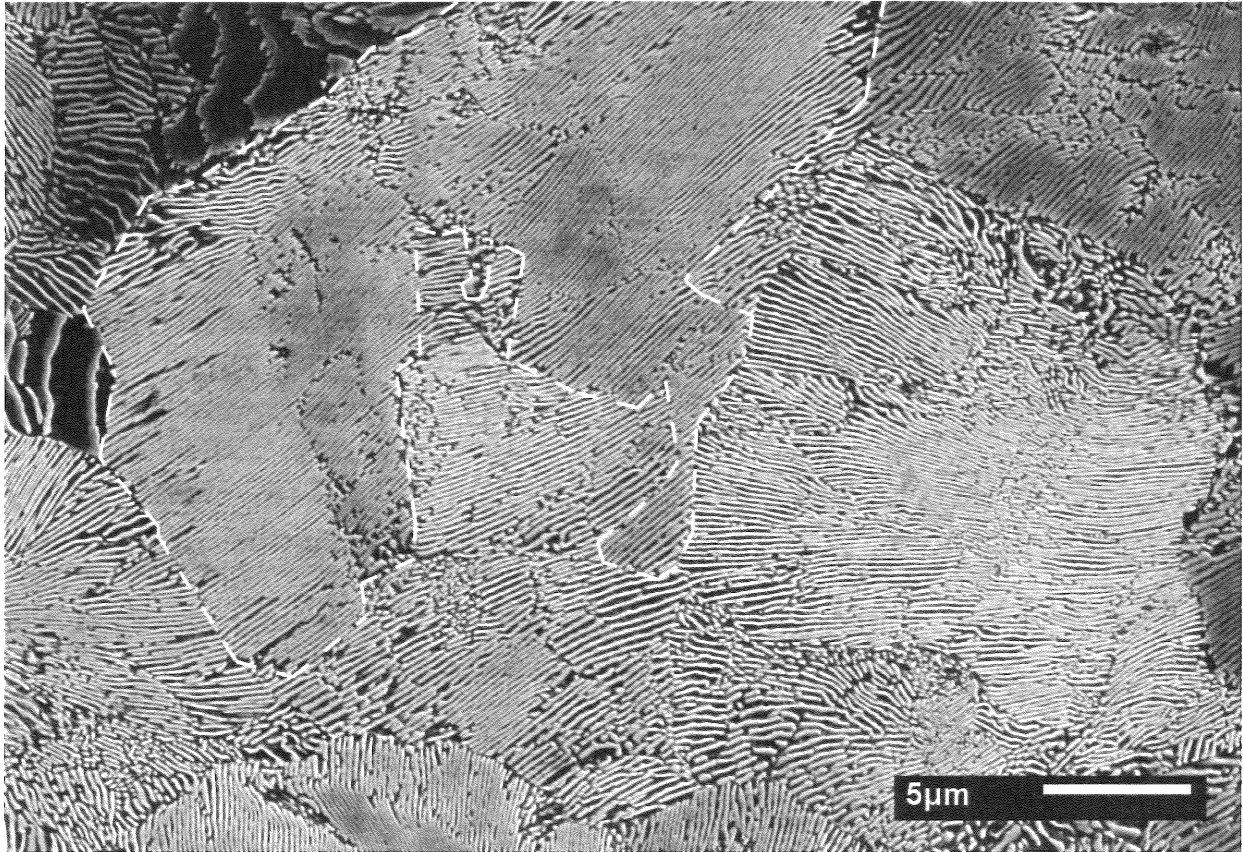
在鍍銀的藍寶石基板上成長氮化鎵，因晶格不匹配所形成的缺陷。

(下方為 SEM 原圖)

作者姓名：蘇誠洲、吳可勵、周易、黃智盟

學校單位：國立交通大學電子物理所

E-Mail：jj2526cc@hotmail.com



作品名稱：奈米侏儸紀 暴龍的入侵

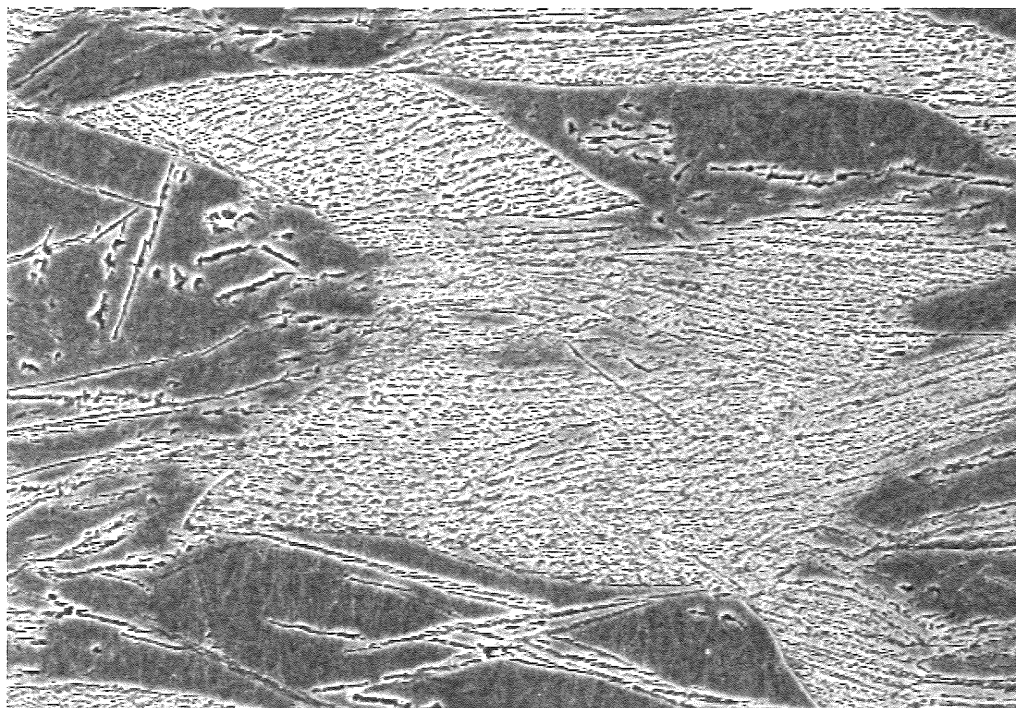
作品內容

超級變韌鐵鋼材在 700°C 恆溫相變態生成極細波來鐵的 SEM 圖。

作者姓名：謝亦傑

學校單位：國立台灣大學材料科學與工程學系

E-Mail：r02527001@ntu.edu.tw



作品名稱：火鳳神鷹

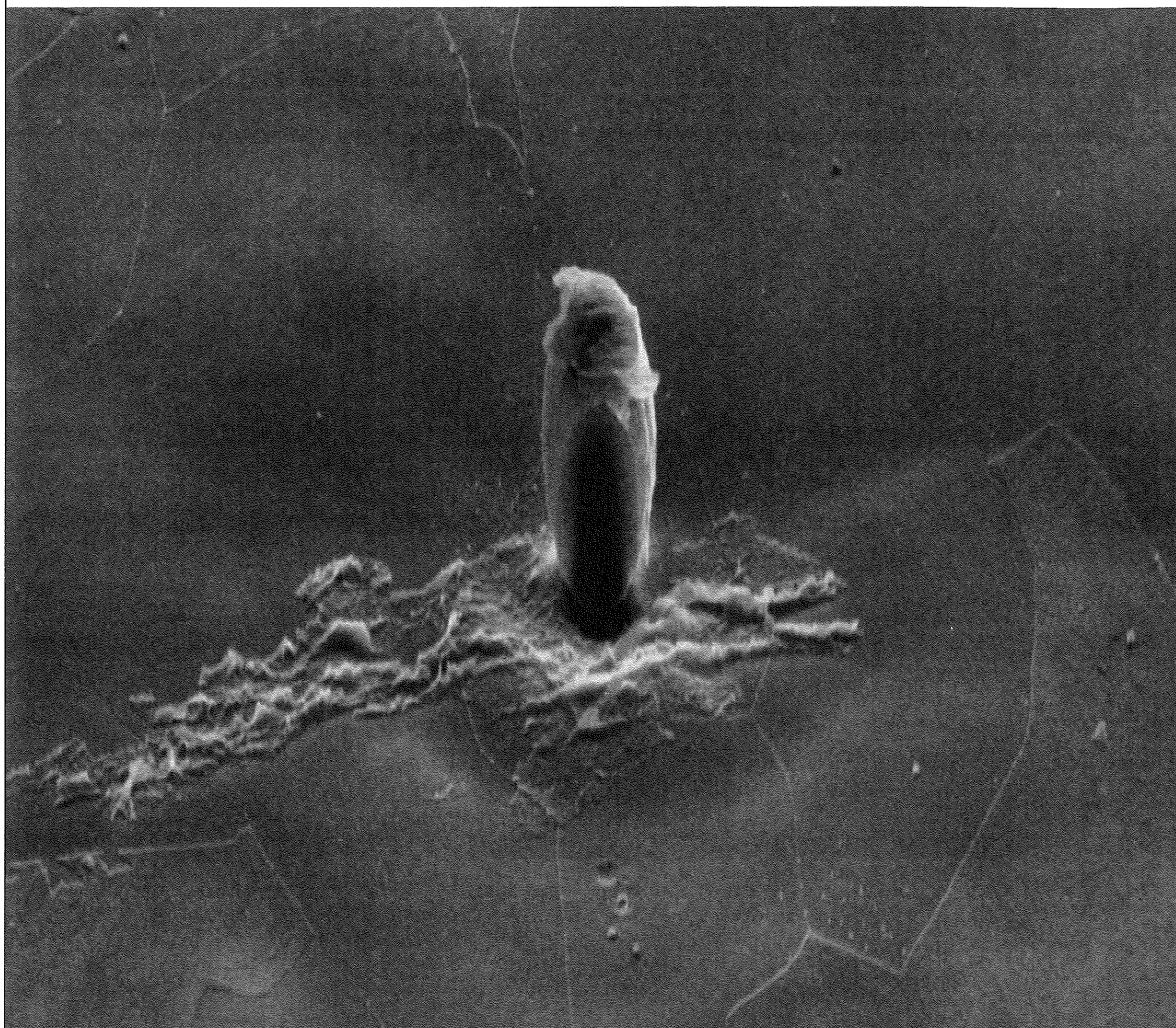
作品內容

傲視群雄，霸氣大鴻展翅，眼神緊盯獵物，伺機而動。

作者姓名：童博彥

學校單位：國立台灣大學材料科學與工程學系

E-Mail：r02527051@ntu.edu.tw



作品名稱：在黑色的大海中竄上的鮭魚

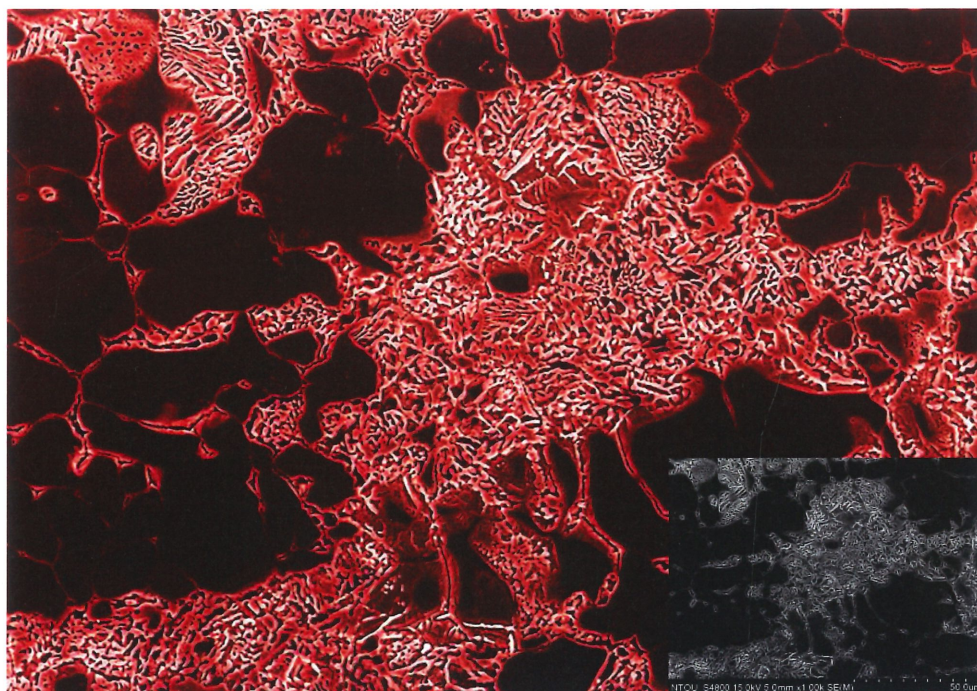
作品內容

試片上的顆粒在 FESEM 的動態對焦下被拉長成一隻長一米六的大鮭魚，躍然於漆黑的海面，撼動著 FESEM 的 5×10^{-5} mbar 的真空。

作者姓名：鄭至閔

學校單位：國立台灣大學材料科學與工程學系

E-Mail：tabonster@gmail.com



作品名稱：腦漿中白色寄生蟲

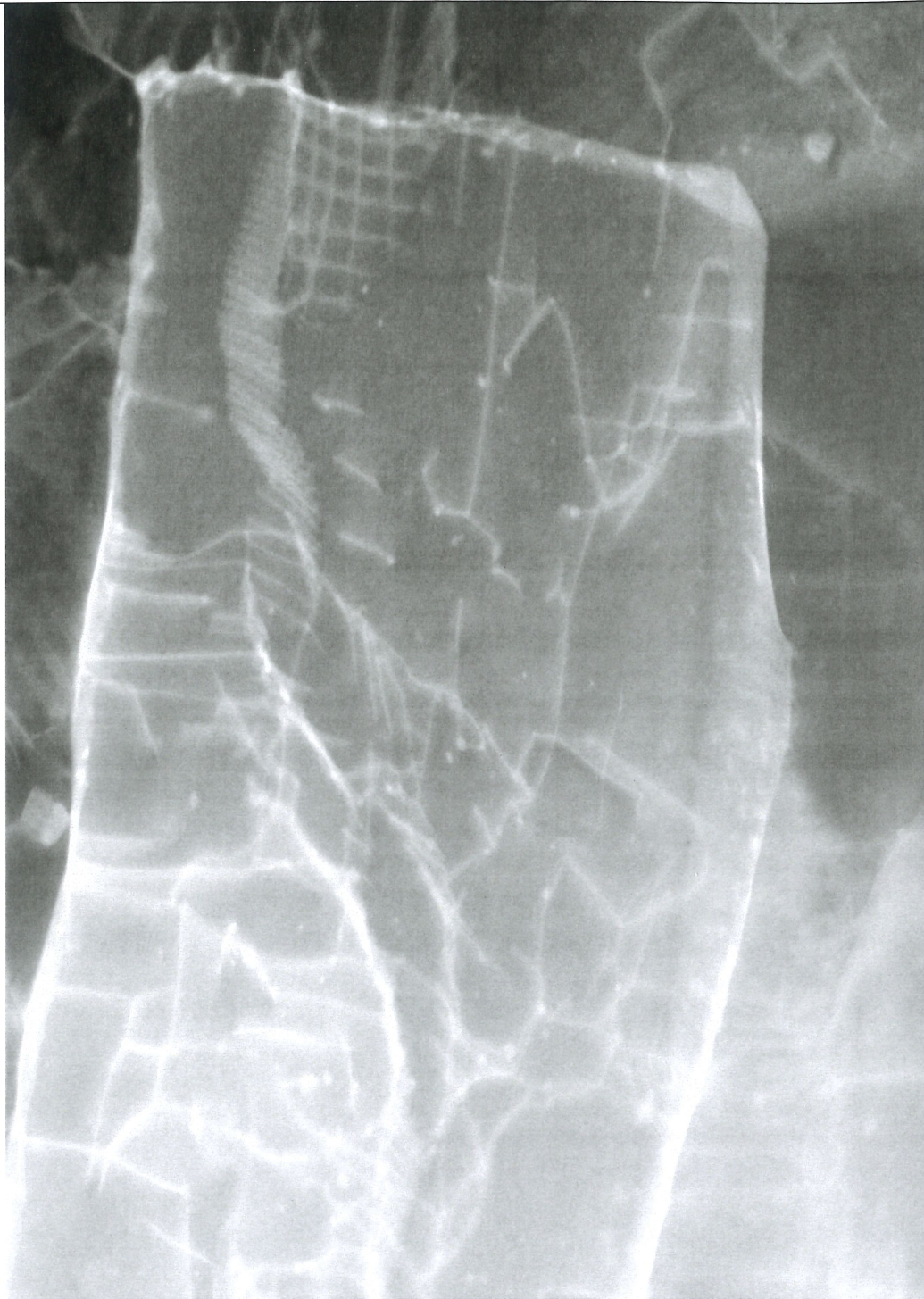
作品內容

雙相不鏽鋼在 750 度熱時效處理後產生共析反應，由 $\alpha \rightarrow \sigma + \gamma'$ 。白色析出相猶如寄生蟲在腦漿裡滋生。

作者姓名：廖敏任

學校單位：國立台灣海洋大學機械與機電所

E-Mail : liao_open@hotmail.com.tw



作品名稱：皇宮中的旋轉樓梯

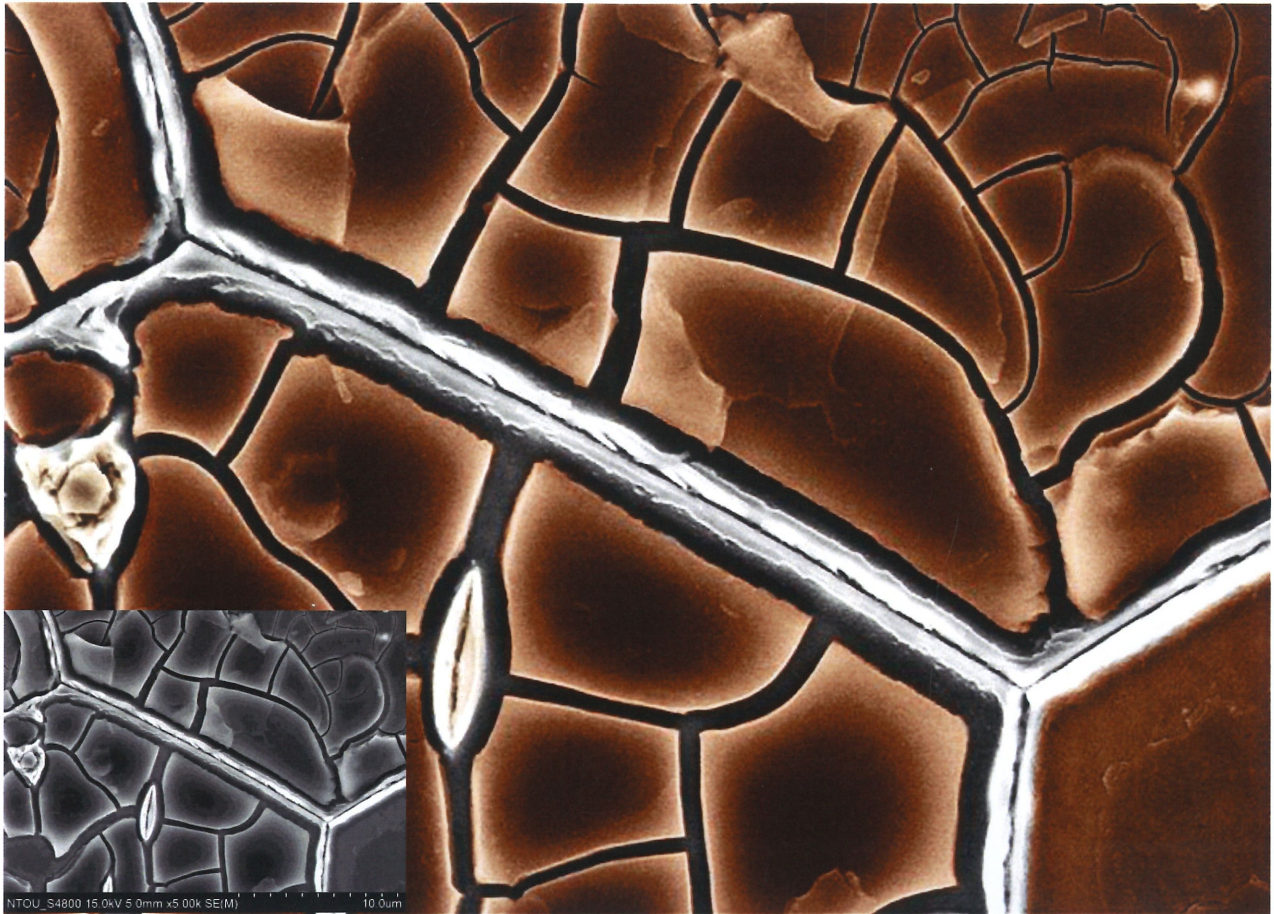
作品內容

由差排在變韌鐵次晶粒內形成螺旋的形狀，就像皇宮中高貴又奢華的樓梯一樣。

作者姓名：陳昱文

學校單位：國立台灣大學材料科學與工程
學系

E-Mail : f01527051@ntu.edu.tw



作品名稱：久旱不雨，稻田龜裂

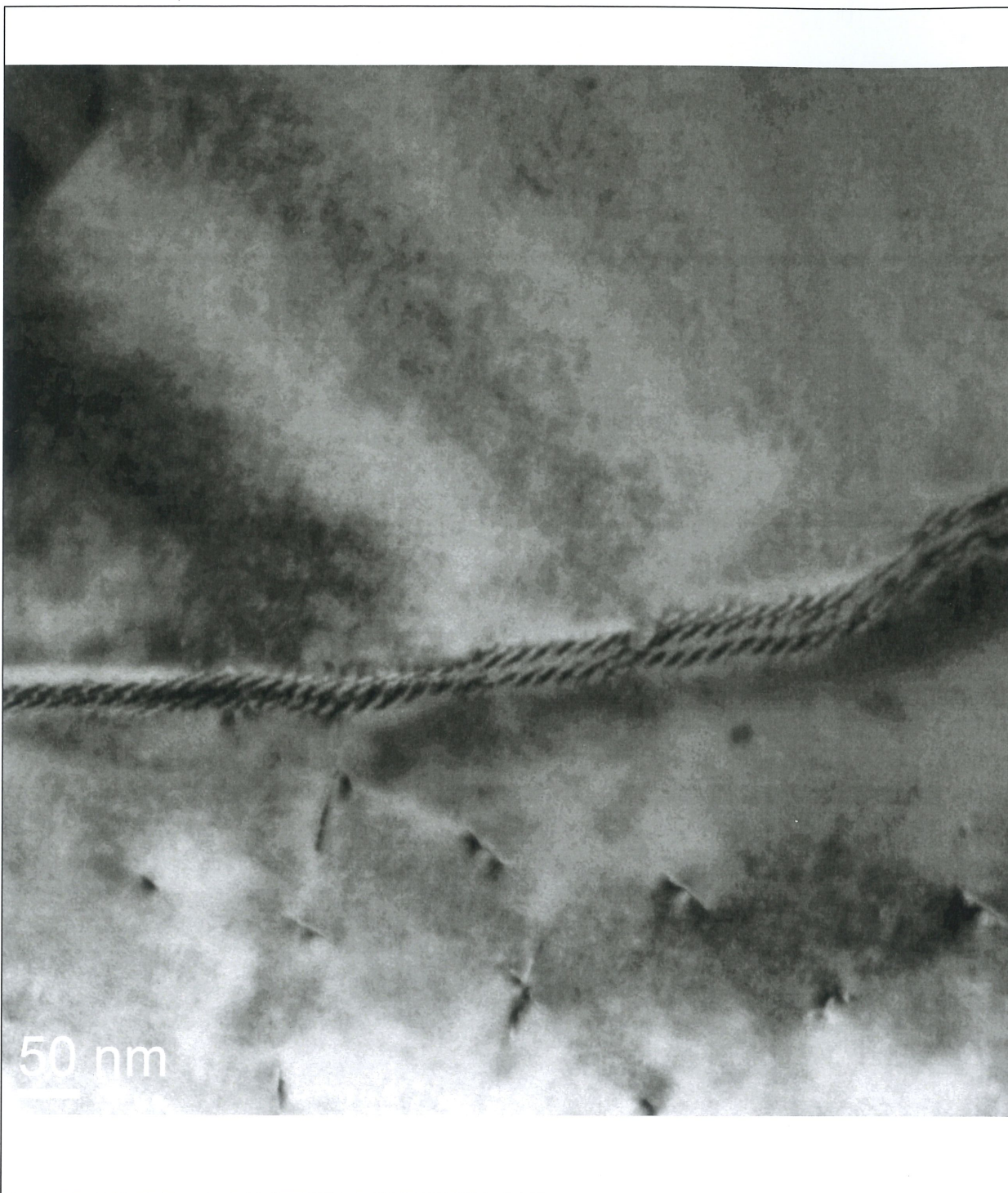
作品內容

雙相不鏽鋼經 600°C-7 小時熱時效處理，龜裂的 α 基地有如乾旱的田地， χ 相在 α/α 晶界析出有如鄉間小路。

作者姓名：林帛江

學校單位：國立臺灣海洋大學 機械與機電所

E-Mail：j2034457@hotmail.com.tw



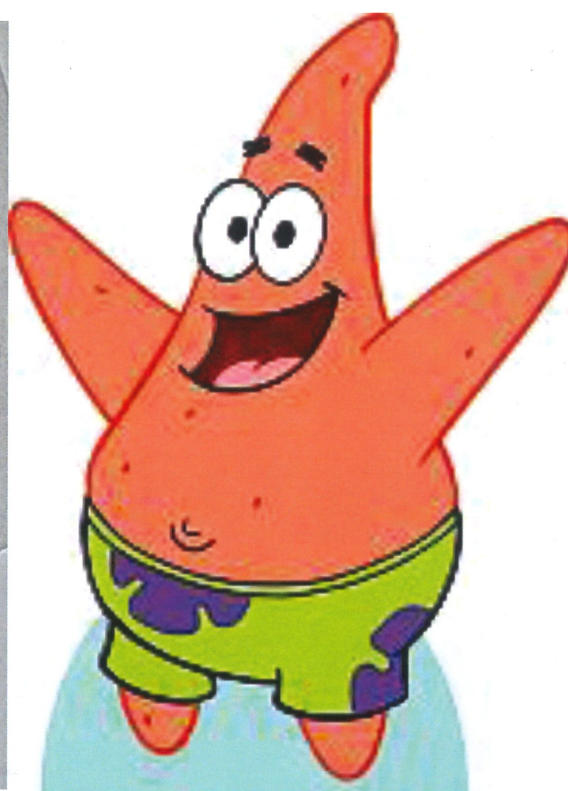
作品名稱：太空天梯

作品內容
鋼鐵中肥粒鐵晶界由差排所構成的形貌，神似穿越宇宙間的太空天梯。

作者姓名：蔡劭璞

學校單位：國立台灣大學材料科學與工程學系

E-Mail： f01527016@ntu.edu.tw



作品名稱：派大星星知我心

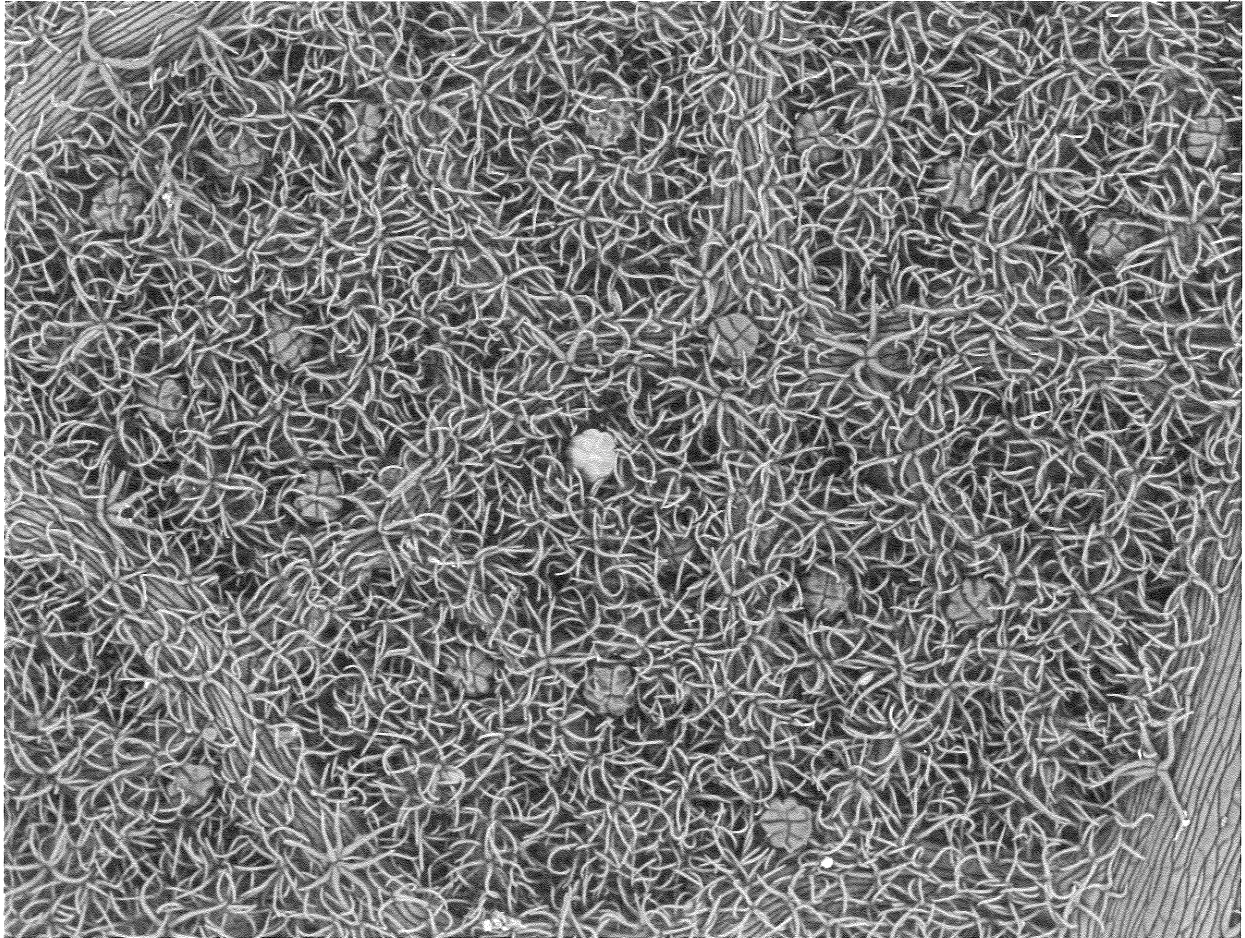
作品內容

水相法合成奈米沸石二維咪唑骨架(ZIF-L)，彼此重疊在穿透顯微鏡下的樣貌。

作者姓名：簡亨達*、李婉綺、康敦彥

學校單位：國立台灣大學化學工程學系

E-Mail：b99504003@ntu.edu.tw



作品名稱：隱藏版美食－梅花糕

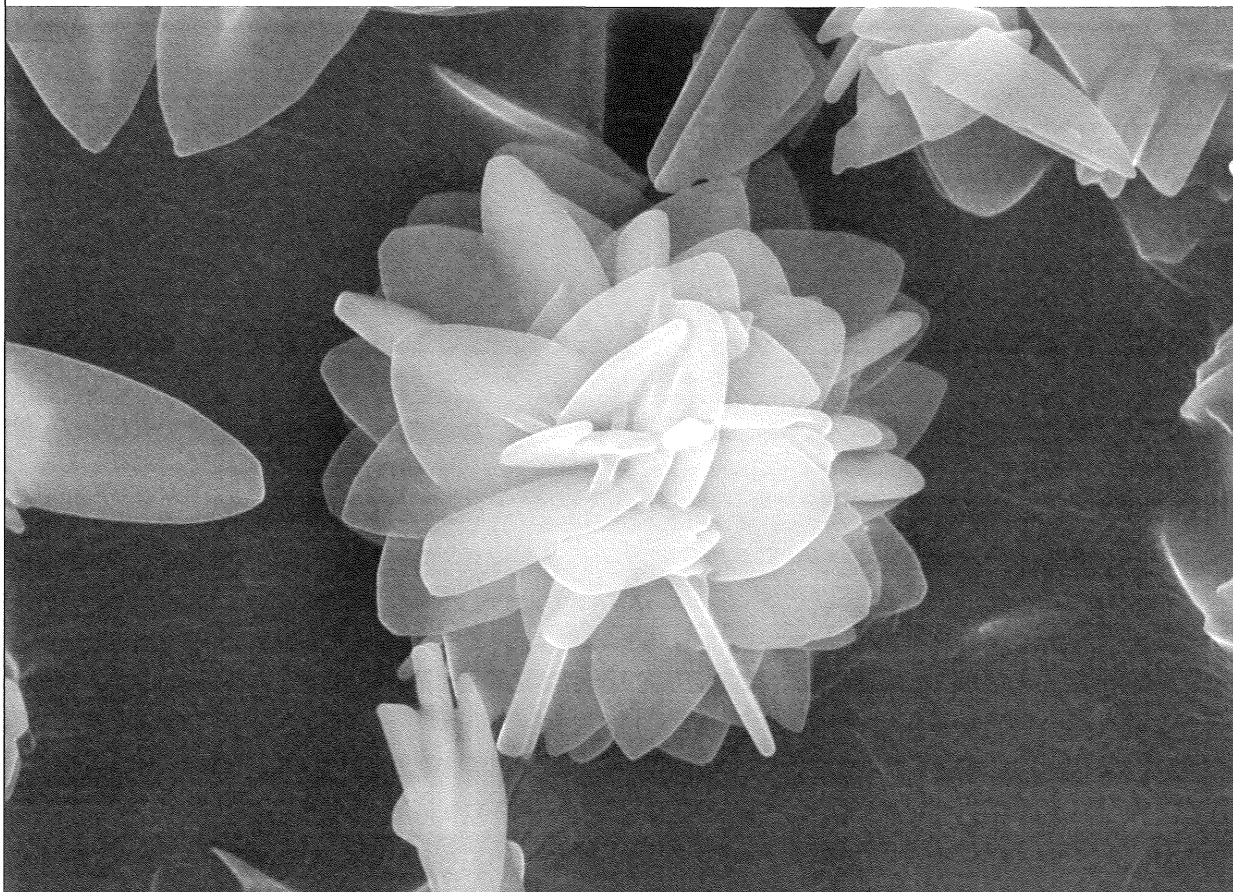
作品內容

粗糠柴葉片下表皮的腺點

作者姓名：李紹輔

學校單位：中興大學生命科學系

E-Mail：g102052023@mail.nchu.edu.tw



作品名稱：蓮花出淤泥而不染

作品內容

利用水相法合成二維沸石咪唑骨架(ZIF-L)，因 inter-growth 而有蓮花狀的結構

作者姓名：王惇平*、李婉綺、康敦彥

學校單位：國立臺灣大學化學工程學系

*E-Mail: r02524044@ntu.edu.tw

CNS SN400YB

SN鋼材 耐震首選

耐震鋼結構 首選SN鋼材 | 簡單鋼結構 更要安全指名CNS SN400YB鋼材 | 鋼材烙印 百分百足重 |



廠房鋼結構：東鋼構 雲林廠



住宅鋼結構：交通大學 蘭花屋



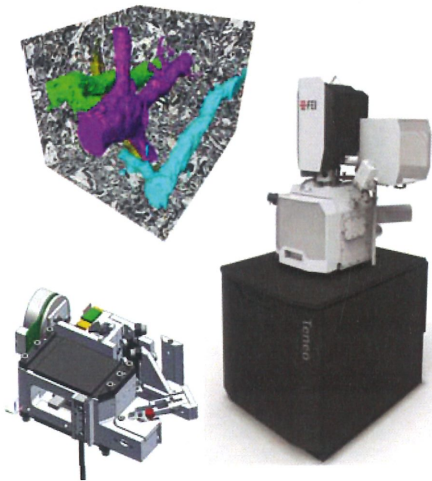
▲日本阪神大地震後，銲接及耐震性能嚴格規範的SN鋼材，是日本唯一認可的耐震鋼結構建築材料。

▲台灣位於環太平洋地震帶，地震發生時，簡單、低矮型鋼結構建物，例如：住宅、商店、廠房、倉庫、車庫、溫室等，往往受創最為嚴重。CNS SN400YB是簡單、低矮型鋼結構建物耐震首選。（交通大學蘭花屋照片由SDE2014大會提供）

▲東和鋼鐵H型鋼獨家鋼材烙印THAS及CNS SN400YB字樣，表示H型鋼百分百足重及永遠的品質保證；相同價格、更高耐震規格。

Volume 3D Imaging for Cell Biology

Two approaches for revealing the ultimate structure

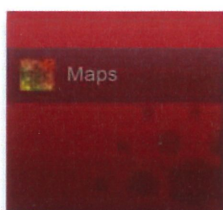


Large area acquisition in 3D by Teneo VS

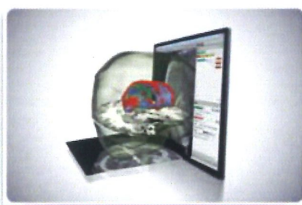
- Large area acquisitions
- Overcoming the limited z-resolution of mechanical slicing by deconvolution
- Exceptional contrast and LoVac performance for challenging samples
- One integrating SW interface to allow ROI targeting by CLEM
- Quick switch between standard SEM use and SBF
- Total solution from FEI, one manufacturer

Volume 3D imaging in high resolution by DualBeam™

- Create 3D imaging of tissue, cell and intracellular organelle in resin embedded samples
- Extended Slice and View enables to create 3D tissue images in high resolution and within a fully automated workflow
- Total solution from 3D imaging to volume rendering
- Compatible with Correlative Workflow
- Total solution from FEI, one manufacturer



MAPS



Amira

Discover More with Maps and Amira
from FEI, One Manufacturer

Learn more @ FEI.com



MICROSYSTEMS

EM Sample Preparation

MATEK The Best R&D Partner

Founded in 1982, Matek Microscopy Technology Inc. (MATEK) is a leading provider of custom electron optics, components and the full range of sample preparation systems for electron microscopy. The company's expertise is in providing high quality, reliable and cost-effective solutions for a wide range of applications in biological, materials and physical sciences.

Our Service Items

- Electron Microscopy
- Electron Spectroscopy
- Electron Tomography
- Electron Spectroscopy
- Electron Spectroscopy
- Electron Spectroscopy

• Contact us, please contact: sales@matek.com / 408-531-6578 ext.3022 / www.matek.com

MATEK The Best R&D Partner

Founded in 1982, Matek Microscopy Technology Inc. (MATEK) is a leading provider of custom electron optics, components and the full range of sample preparation systems for electron microscopy. The company's expertise is in providing high quality, reliable and cost-effective solutions for a wide range of applications in biological, materials and physical sciences.

Our Service Items

- Electron Microscopy
- Electron Spectroscopy
- Electron Tomography
- Electron Spectroscopy
- Electron Spectroscopy
- Electron Spectroscopy

• Contact us, please contact: sales@matek.com / 408-531-6578 ext.3022 / www.matek.com

MATEK The Best R&D Partner

Founded in 1982, Matek Microscopy Technology Inc. (MATEK) is a leading provider of custom electron optics, components and the full range of sample preparation systems for electron microscopy. The company's expertise is in providing high quality, reliable and cost-effective solutions for a wide range of applications in biological, materials and physical sciences.

Our Service Items

- Electron Microscopy
- Electron Spectroscopy
- Electron Tomography
- Electron Spectroscopy
- Electron Spectroscopy
- Electron Spectroscopy

• Contact us, please contact: sales@matek.com / 408-531-6578 ext.3022 / www.matek.com

BIO AR-TEK

Bio Materials Analysis Technology Inc. (Bio MATEK) utilizes the most advanced tools in the physical and chemical characterization of materials in biological systems. Bio MATEK offers a wide range of R&D sample preparation and analysis services, including the preparation of analytical samples following the recommendations in ISO 9001:2015.

Liquid Sample TEM

- Liquid Sample TEM Service and Sales
- Biological and Biomaterials EM Specimen Preparation
- Other Electron Microscopy Analysis: Liquid - Cryo - Gels - Solid - etc.

BIO AR-TEK

Bio Materials Analysis Technology Inc. (Bio MATEK) utilizes the most advanced tools in the physical and chemical characterization of materials in biological systems. Bio MATEK offers a wide range of R&D sample preparation and analysis services, including the preparation of analytical samples following the recommendations in ISO 9001:2015.

Liquid Sample TEM

- Liquid Sample TEM Service and Sales
- Biological and Biomaterials EM Specimen Preparation
- Other Electron Microscopy Analysis: Liquid - Cryo - Gels - Solid - etc.

BIO AR-TEK

Bio Materials Analysis Technology Inc. (Bio MATEK) utilizes the most advanced tools in the physical and chemical characterization of materials in biological systems. Bio MATEK offers a wide range of R&D sample preparation and analysis services, including the preparation of analytical samples following the recommendations in ISO 9001:2015.

Liquid Sample TEM

- Liquid Sample TEM Service and Sales
- Biological and Biomaterials EM Specimen Preparation
- Other Electron Microscopy Analysis: Liquid - Cryo - Gels - Solid - etc.

EM UC7/FC7
Ultramicrotome



EM GP
Plunge Freezer

MATEK The Best R&D Partner

Founded in 1982, Matek Microscopy Technology Inc. (MATEK) is a leading provider of custom electron optics, components and the full range of sample preparation systems for electron microscopy. The company's expertise is in providing high quality, reliable and cost-effective solutions for a wide range of applications in biological, materials and physical sciences.

Our Service Items

- Electron Microscopy
- Electron Spectroscopy
- Electron Tomography
- Electron Spectroscopy
- Electron Spectroscopy
- Electron Spectroscopy

• Contact us, please contact: sales@matek.com / 408-531-6578 ext.3022 / www.matek.com

BIO AR-TEK

Bio Materials Analysis Technology Inc. (Bio MATEK) utilizes the most advanced tools in the physical and chemical characterization of materials in biological systems. Bio MATEK offers a wide range of R&D sample preparation and analysis services, including the preparation of analytical samples following the recommendations in ISO 9001:2015.

Liquid Sample TEM

- Liquid Sample TEM Service and Sales
- Biological and Biomaterials EM Specimen Preparation
- Other Electron Microscopy Analysis: Liquid - Cryo - Gels - Solid - etc.

EM PACT2 / RTS
High Pressure Freezer



EM AFS2 / FSP
Freeze Substitution System



EM CPD300
Critical Point Dryer



EM TRIM2
Automatic Specimen Trimmer



EM TIC 3X
Triple Ion Beam Slope Cutter



EM TP
Tissue Processor



EM ACE200/600
Sputter Coater



EM AC20
Automated Grid Stainer

EM KMR3
Glass Knife Maker

EM TXP
Target Surfacing System

台灣總代理

友聯光學有限公司

地址：新北市汐止區新台五路1段81號4樓之3

電話：02-26980508

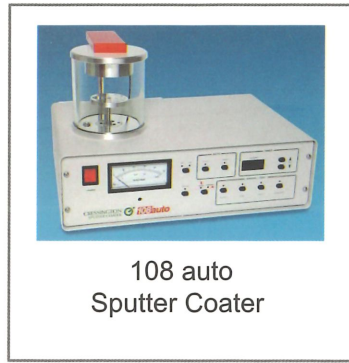
E-mail：unionopt@ms11.hinet.net

網址：http://www.unionoptical.com.tw/

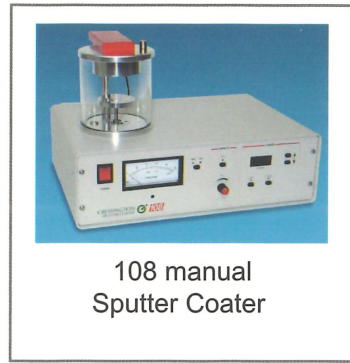
Sputter Coater



208HR High Resolution
Sputter Coater
for FE-SEM



108 auto
Sputter Coater



108 manual
Sputter Coater

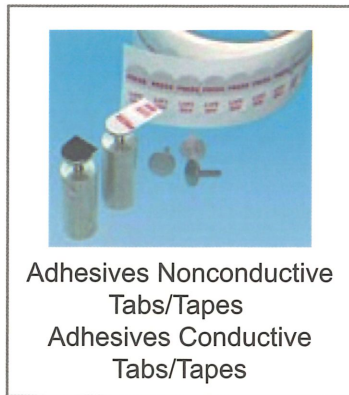


Targets for
Sputter Coaters

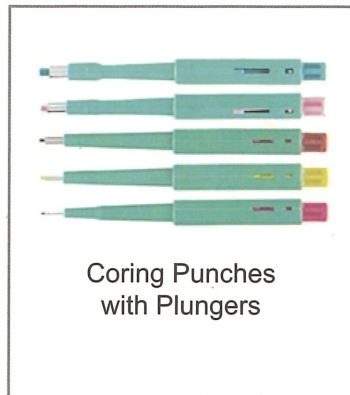
Supplies / Accessories



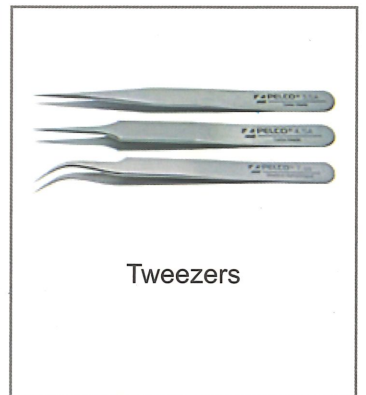
Adhesives
Conductive SEM
Nonconductive



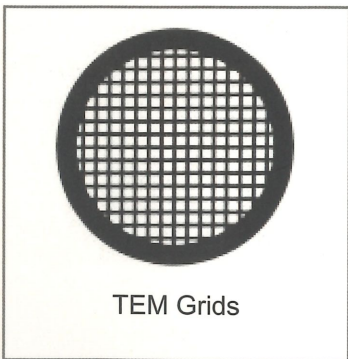
Adhesives Nonconductive
Tabs/Tapes
Adhesives Conductive
Tabs/Tapes



Coring Punches
with Plungers



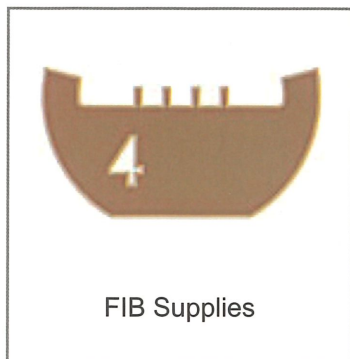
Tweezers



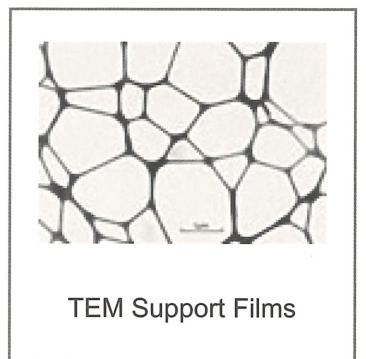
TEM Grids



TEM Grid
Storage Boxes

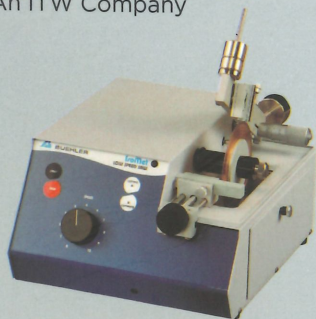


FIB Supplies



TEM Support Films

電顯試片前製備儀器及耗材



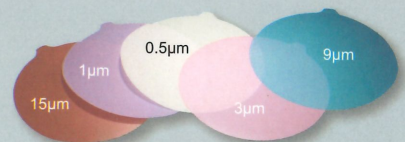
IsoMet
慢速精密切割機



EcoMet 250
微電腦控制研磨拋光機



MasterMet
二氧化矽最終拋光懸浮液



鑽石拋光膜 (鑽石砂紙)

Transmission Electron Microscopy Study to High-k Hafnium Oxide Film for Application in Backside Illumination CMOS Image Sensor

Yi-Chang Li (李奕鋈) and Chuan-Pu Liu (劉全璞)*

Department of Materials Science and Engineering, National Cheng Kung University, Taiwan
*cpliu@mail.ncku.edu.tw

BSI (backside illumination) sensor technology has gradually become popular for smaller pixel image sensors owing to its high sensitivity, although BSI sensors suffer from high dark currents due to backside surface damage [1]. Using high k films is a solution to suppress dark current. Choosing an optimized high k dielectric film with negative charges can induce such a positive electric field at silicon surface that traps carriers from silicon interface. The commonly used high k dielectrics include HfO_x due to its high k value and negative charge property. In the proceeding procedures, the HfO_x films with different thickness are coated by ALD (atomic layer deposition) method on the p-Si for comparison. TEM (Transmission Electron Microscopy) was used to examine microstructure of each interface and layers and correlates with the CV (Capacitance voltage) measurement results.

Reference

1. H. Watanabe *et al.*, "A 1.4 μm Front-Side Illuminated Image Sensor with Novel Light Guiding Structure Consisting of Stacked Lightpipes," IEEE, IEDM11, 179-182 (2011)

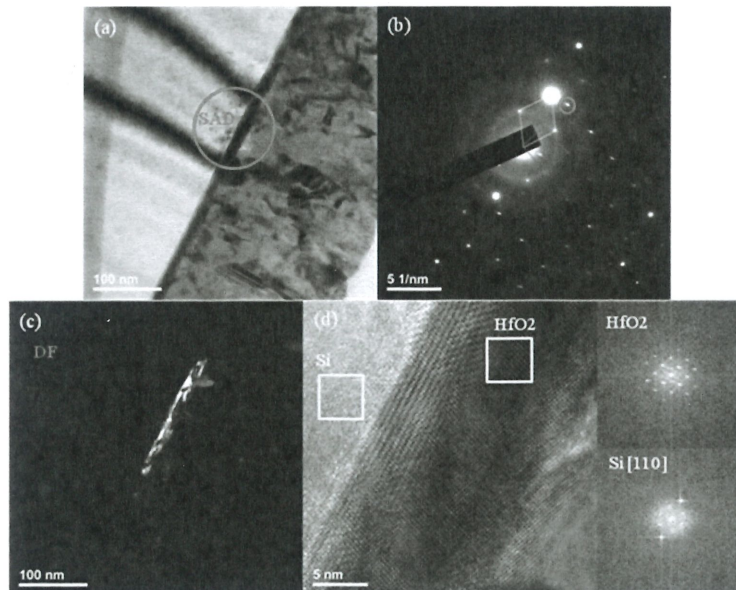


Figure 1. (a) Low magnification TEM image, (b) Selected area diffraction pattern, (c) Dark field image, and (d) HRTEM image for the 12 nm thick HfO_x layer sample (the corresponding FFT transform patterns in the inset coming from the yellow boxes).